JENNI KOTILA

MICROSCOPIC NUCLEAR-STRUCTURE CALCULATIONS FOR THE LOW-LYING COLLECTIVE STATES IN EVEN-EVEN NUCLEI

DEPARTMENT OF PHYSICS,
UNIVERSITY OF JYVÄSKYLÄ
RESEARCH REPORT No. 5/2008

MICROSCOPIC NUCLEAR-STRUCTURE CALCULATIONS FOR THE LOW-LYING COLLECTIVE STATES IN EVEN-EVEN NUCLEI

BY

JENNI KOTILA

Academic Dissertation
for the Degree of
Doctor of Philosophy

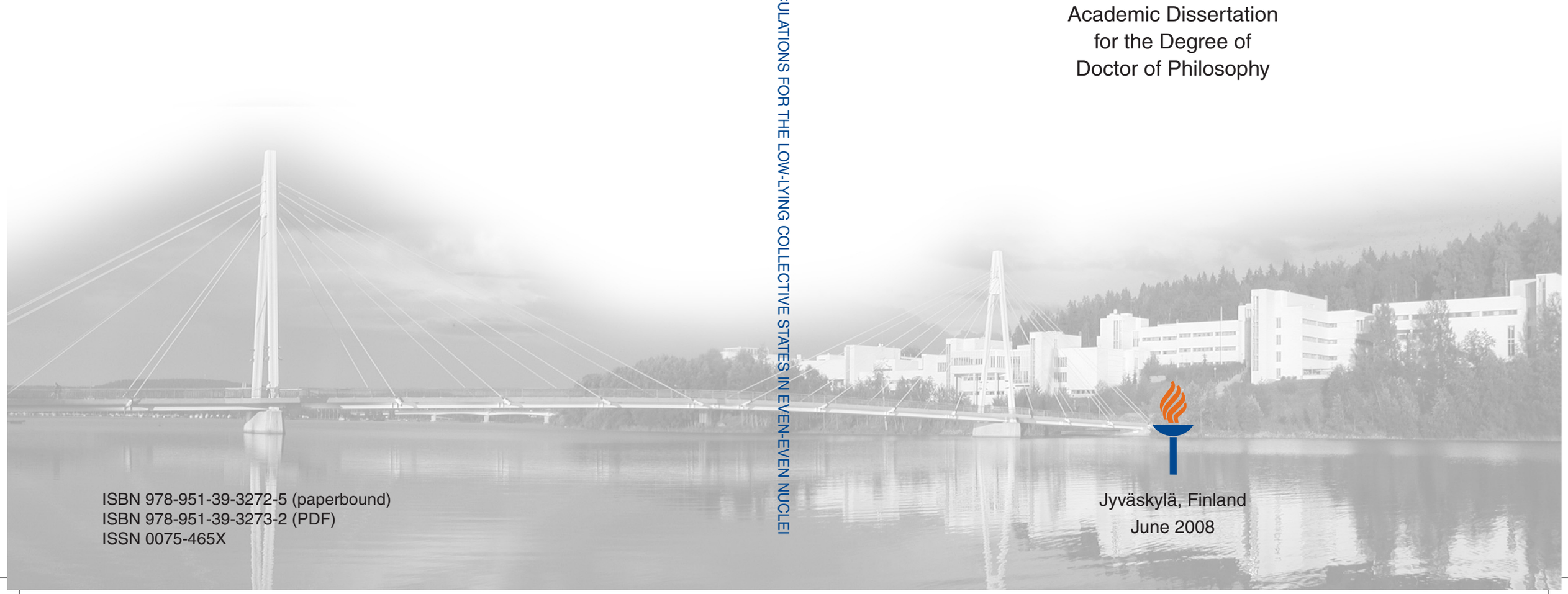

ISBN 978-951-39-3272-5 (paperbound)
ISBN 978-951-39-3273-2 (PDF)
ISSN 0075-465X

Jyväskylä, Finland
June 2008

DEPARTMENT OF PHYSICS
UNIVERSITY OF JYVÄSKYLÄ
RESEARCH REPORT No. 5/2008

MICROSCOPIC NUCLEAR-STRUCTURE CALCULATIONS FOR THE LOW-LYING COLLECTIVE STATES IN EVEN-EVEN NUCLEI

BY
JENNI KOTILA

Academic Dissertation
for the Degree of
Doctor of Philosophy

To be presented, by permission of the
Faculty of Mathematics and Natural Sciences
of the University of Jyväskylä,
for public examination in Auditorium FYS-1 of the
University of Jyväskylä on June 18, 2008
at 12 o'clock noon

Jyväskylä, Finland
June 2008

ABSTRACT

In this thesis work the low-energy collective spectra of spherical or nearly spherical nuclei have been studied by means of the Microscopic Anharmonic Vibrator Approach (MAVA). The adopted theory is based on a large single-particle valence space and a realistic nuclear Hamiltonian using phenomenologically renormalized two-body interaction based on the Bonn one-boson-exchange G-matrix. The used theoretical formalism naturally embraces vibrational degrees of freedom starting from the quasiparticle random-phase approximation (QRPA) collective phonons. The above mentioned nuclear Hamiltonian is used to introduce anharmonicities into the description of the low-lying excited states leading to dynamical splitting of the energies of the two-phonon vibrational states. At the same time the Hamiltonian is also allowed to mix the one-phonon and two-phonon collective degrees of freedom.

A systematic investigation of the reduced electric quadrupole decay probabilities and level energies of even-even $^{94-100}$Mo, $^{98-106}$Ru and $^{110-120}$Cd isotopes is performed using the MAVA. Some large scale calculations have also been done in the aim to fix the free parameters by experimental data so that a large region of nuclei could be studied with the same parameters. This is done by modifying the MAVA to allow user friendly calculations globally by choosing vibrational type of nuclei from the entire chart of nuclei.

This thesis is divided in two different parts, an introductory part and five publications. The introductory part provides a summary of the topics related to the publications and gives a more detailed overview of the different aspects of the performed studies supplemented with references.

Author

Jenni Kotila
Department of Physics
University of Jyväskylä
Finland

Supervisor

Professor Jouni Suhonen
Department of Physics
University of Jyväskylä
Finland

Reviewers

Professor Peter Schuck
Groupe de Physique Théorique
Institut de Physique Nucléaire
France

Dr. Roberto Liotta
Department of Physics
Royal Institute of Technology (KTH)
AlbaNova University Center
Sweden

Opponent

Professor Francesco Iachello
Department of Physics
Yale University
USA

PREFACE

The work reviewed in this thesis has been carried out at the Department of Physics of the University of Jyväskylä during the years 2003-2008.

I wish to thank my supervisor professor Jouni Suhonen for an interesting research topic and all the guidance. I am also grateful to Dr. Doru Delion and Dr. Johannes Hopiavuori whose guidance and help have been of great importance to me. The opportunities to attend conferences, seminars and summer schools, both in Finland and abroad, are also gratefully acknowledged. They have given a lot of new points of view and have provided great possibilities to meet scientists from all around the world. They have also helped in establishing personal contacts and gaining experience of sharing the scientific work with colleagues. At this point I would also like to thank all the people of the theoretical nuclear physics group.

The atmosphere of the Department of Physics has already been praised in many other prefaces of PhD. theses. I sincerely agree with this praise and take the opportunity to thank all the people with whom I have worked with.

The financial support from the Department of Physics of the University of Jyväskylä, the rector of the University of Jyväskylä and the Graduate School of Particle and Nuclear Physics are gratefully acknowledged.

Finally, I would like to thank my husband Pekka, my parents and my siblings for all the love and encouragement.

Jyväskylä, May 2008
Jenni Kotila

CONTENTS

LIST OF INCLUDED ARTICLES

PI J. Kotila, J. Suhonen and D.S. Delion, *Microscopic calculation of the electric decay properties of low-lying vibrational states in even* $^{110-120}$*Cd isotopes*, Phys. Rev. C **68** (2003) 014307

PII J. Kotila, J. Suhonen and D.S. Delion, *Low-lying collective states in* $^{98-106}$*Ru isotopes studied using a microscopic anharmonic vibrator approach*, Phys. Rev. C **68** (2003) 054322

PIII J. Kotila, J. Suhonen and D.S. Delion, *Study of the low-lying collective states in* $^{94-100}$*Mo isotopes using the MAVA*, Nucl. Phys. A **765** (2006) 354

PIV J. Kotila, J. Suhonen and D.S. Delion, *Study of the low-lying collective states using a Microscopic Anharmonic Vibrator Approach*, Czech. J. Phys. **56** (2006) 473

PV J. Kotila, J. Suhonen and D.S. Delion, *Analysis of the low-lying collective states using the MAVA*, Collective Motion and Phase Transitions in Nuclear Systems, Proceedings of the Predeal International Summer School in Nuclear Physics, Predeal , Romania 28 August-9 September 2006, Eds. A.A. Raduta, V. Baran, A.C. Gheorghe and I.Ursu (World Scientific, 2007) 271-283

The author of this thesis has written the publication **PV**, and part of the publications **PI**, **PII**, **PIII** and **PIV**, and has done all the calculations.

1 INTRODUCTION

Nuclear physics is a subject of enduring interest and importance. The atomic nucleus is a fascinating and unique example of a quantum system of relatively few particles displaying both single-particle and collective motions, and it is governed by three out of the four fundamental forces of nature, namely, the electromagnetic, the strong nuclear and the weak interactions. The radiation from nuclei have found many applications in a wide range of fields.

Nuclear physics is still in many respects an experimental subject: even though the nucleus has been studied for a century, new phenomena are continually being found. What we know is still conditioned by the precision and limitations of the available equipment and we do not yet have a simple and comprehensive theory of the nucleus. To describe it we have to rely on models that each describe certain aspects of nuclear structure, and they often do this with great accuracy and sophistication.

The purpose of the present work is to study low-lying collective states with vibrational-type behaviour. These states lie below the pairing gap which is produced by the short-range nucleon correlations whereas the collectivity of the states is due to the long-range residual interaction. These collective states have been investigated in various ways, both experimentally and theoretically, as collective phonons and their multiples. The phenomenological models study these latter mentioned multiphonon states and anharmonicities associated with them in terms of pure phonons. Probably the most famous of such models is the interacting boson model (IBM) [1] which has proved to be a powerful tool for providing systematics of the low-energy multiphonon spectra and clarifying their gross features.

In order to explain multiphonon states microscopically, one has to go beyond

Tamm-Dancoff (TDA) or random-phase approximation (RPA) [2, 3] which, by their own nature, cannot account for anharmonicities. The anharmonic features can be accounted for e.g., by the use of the multistep shell model (MSM) [4, 5, 6, 7] or the multiphonon model (MPM) [8, 9, 10, 11]. Both methods generate a set of multiphonon states out of the TDA or RPA phonons.

In Ref. [12] an exact formulation and solution of the nuclear eigenvalue problem in a microscopic multiphonon space is proposed starting from a TDA phonon. It is stated that the method can be be reformulated to include RPA phonons but that extension could be unnecessary because the method already in its present TDA formulation yields an explicitly correlated ground state. However, the use of quasiparticles instead of particle-hole states would be especially useful allowing to study multiphonon spectra in open shell spherical and deformed nuclei not easily accessible to standard shell model

Another method for the microscopic description of multiphonon states is the quasiparticle-phonon model (QPM) [13] which has been used to study a large variety of spectra for vibrational as well as for deformed nuclei [14, 15, 16, 17, 18, 19, 20]. In the QPM the wave function is built in a similar way as done in the MSM, but the equations of motion are derived from a different principle.

It is also possible to extend the particle hole basis by a direct inclusion of the two-particle-two-hole terms within the extended quasiparticle random-phase approximation [21] but the resulting equations are rather complicated. In the second RPA only the 1p-1h and 1h-1p components of the one-body amplitudes and the 2p-2h and 2h-2p of the two-body amplitudes are taken into account. However, in Ref. [22] it is found that only extended RPAs with all one-body and two-body amplitudes give zero excitation energy to the double-phonon state corresponding to the spurious mode associated with the translational motion. In most applications it is preferred, for the sake of simplicity, to adopt the multistep technique in which building blocks are the quasiparticle random-phase approximation (QRPA) phonons. The multistep technique is also adapted in the MAVA formalism, the subject of this thesis work.

In the first step of the MAVA the low-energy collective phonons of the open-shell nuclei are described within the framework of the QRPA. The QRPA describes harmonic small-amplitude vibrations around a spherical nuclear shape leading to collective low-energy solutions of the QRPA equations. In the second step of the MAVA more complicated structures are constructed by combining these one-phonon states to two-phonon states and letting one-phonon and two-phonon states interact among each other through the residual two-body Hamiltonian.

2 THE MICROSCOPIC ANHARMONIC VIBRATOR APPROACH

The method for the microscopic description of the structure of nuclei with two-phonon states is outlined in this section. The concept of BCS quasiparticle is introduced to handle the pairing interaction in a nucleus. The excitations of an even-even nucleus are formed by first calculating the QRPA phonons and then using these phonons as building blocks for more complicated structures.

The collective low-lying excitations in even-even nuclei are described in terms of single-particle eigenstates in a given spherically symmetric mean-field. These states are labeled by spherical single-particle quantum numbers, i.e., isospin, energy eigenvalue, orbital angular momentum, total spin and its z-projection, τ, ϵ, l, j and m, respectively. For simplicity the following shorthand notation is used: $\tau\epsilon ljm \rightarrow \tau jm$, where j now absorbs the energy eigenvalue and orbital angular momentum. The isospin index is dropped whenever its presence is unambiguously understood. The following notation is also found to be useful: $\tilde{c}_{jm} \equiv (-1)^{j+m} c_{j-m}$. Exploiting these notations, the creation and annihilation operators corresponding to state $\tau\epsilon jm$ are written as $c^{\dagger}_{\tau jm}$ and $c_{\tau jm}$ respectively.

2.1 The nuclear mean-field and residual interaction

The problem of treating the dynamics of an atomic nucleus is a challenge for theorists to solve. On one hand the application of exact methods is out of the question since the number of particles involved is far too large for that. On the other hand,

the number of particles involved is not sufficiently large for the use of statistical methods. To make the description even more difficult, the nucleons feel the presence of a strong mutual attraction, leading to bound nuclei despite the Coulomb repulsion between the protons.

The microscopic nuclear Hamiltonian, given in terms of the occupation number representation [23], can be separated into two terms, the single-particle kinetic energy term and the two-body interaction:

$$\begin{aligned} H &= \sum_{j_1 m_1} \epsilon_{j_1} c^{\dagger}_{j_1 m_1} c_{j_1 m_1} + \sum_{j_i m_i, i=1,\ldots,4} \overline{v}_{j_1 m_1 j_2 m_2 j_3 m_3 j_4 m_4} c^{\dagger}_{j_1 m_1} c^{\dagger}_{j_2 m_2} c_{j_4 m_4} c_{j_3 m_3} \\ &\equiv H_{\mathrm{SP}} + H_{\mathrm{I}}. \end{aligned} \tag{1}$$

The antisymmetrized two-body interaction matrix element $\overline{v}_{j_1 m_1 j_2 m_2 j_3 m_3 j_4 m_4}$ is defined by

$$\overline{v}_{j_1 m_1 j_2 m_2 j_3 m_3 j_4 m_4} \equiv v_{j_1 m_1 j_2 m_2 j_3 m_3 j_4 m_4} - v_{j_1 m_1 j_2 m_2 j_4 m_4 j_3 m_3}, \tag{2}$$

where

$$v_{j_1 m_1 j_2 m_2 j_3 m_3 j_4 m_4} = \int \phi^{\dagger}_{j_1 m_1}(\mathbf{x}) \phi^{\dagger}_{j_2 m_2}(\mathbf{x'}) v(\mathbf{r,r'}) \phi_{j_3 m_3}(\mathbf{x}) \phi_{j_4 m_4}(\mathbf{x'}) d^3\mathbf{r} d^3\mathbf{r'} \tag{3}$$

and $\phi_{j_1 m_1}(\mathbf{x})$ is a mean-field single-particle wave function containing the radial coordinate $\mathbf{r}$ and spin $\mathrm{s} = \frac{\mathbf{1}}{\mathbf{2}}$, i.e., $\mathbf{x} = (\mathbf{r,s})$.

In the mean-field approximation, MFA, the assumption is made that each nucleon is moving independently in an average field caused by the other nucleons. This external, so called mean-field potential V_{MF}, is constructed to simulate the total effect of the surrounding nuclear matter as well as possible. The task is to find an optimal form of V_{MF} making the matrix elements of the residual interaction H_{RES}, defined by

$$H = \underbrace{H_{\mathrm{SP}} + V_{\mathrm{MF}}}_{H_{\mathrm{MF}}} + \underbrace{H_{\mathrm{I}} - V_{\mathrm{MF}}}_{H_{\mathrm{RES}}}, \tag{4}$$

small. One way to accomplish this goal, i.e., to find the correct form of V_{MF}, is to use the iterative Hartree-Fock method. By doing this, a system of strongly interacting particles is converted to that of weakly interacting mean-field quasiparticles occupying the mean-field single-particle orbitals. V_{MF} can also be approximated as a harmonic oscillator potential or some more realistic phenomenological potential like Woods-Saxon potential with its parametrization given by, e.g., Bohr and Mottelson [24].

The many-body problem of the nucleus is simplified by the introduction of the mean-field. For some nuclei this means even that we can describe certain nuclear properties, like the magnetic moment, in single-particle terms. This is the case, for instance, for nuclei with just one particle or hole outside a closed major shell or a particle-hole excitation on a major shell of fully occupied single-particle orbitals. Naturally these cases are rare and for general cases a proper inclusion of the residual interaction H_{RES} is needed to obtain realistic results.

2.2 The BCS and quasiparticles

The nucleon pairs tend to favour coupling to total angular momentum zero. This short-range nuclear force is called the nuclear pairing, and is the most prominent component of the residual interaction. It was first Mayer [25, 26] who pointed out that for all the even-even nuclei the spin and parity of the ground state, $J^{\pi}_{\mathrm{g.s.}}$, equals to 0^{+}. The pairing effect was then introduced to explain this feature.

Within the most general case of n particles an exact treatment is no longer possible and different approximation methods to obtain the nuclear pair distribution have been introduced: generalized seniority [27] (GS), broken-pair approximation [28] (BPA), Bardeen-Cooper-Schrieffer theory [29] (BCS), to mention some. The BCS method has been adopted from the theory of superconductivity and was first proposed to be used in the nuclear environment by Bohr, Mottelson and Pines [30]. The BCS approach describes the ground state of an even-even nucleus as being in a kind of superconducting phase. This means that all the nucleons have been coupled pairwise to zero angular momentum to form a Cooper pair condensate of boson-like objects.

The BCS ground state is written as linear combination of states with different numbers of nucleon pairs:

$$|BCS\rangle = \prod_{jm>0} (u_j - v_j c^{\dagger}_{jm} \tilde{c}^{\dagger}_{jm})|core\rangle, \tag{5}$$

where the state $|core\rangle$ denotes the inert core, taken as effective particle vacuum: $c_{jm}|core\rangle = 0$ for all jm. The core consists of occupied mean-field orbitals that can be neglected to first approximation in the calculations. The coefficients u_j and v_j are called the unoccupation and occupation amplitudes, respectively.

The BCS ground state has no exact particle number, i.e., it is not an eigenstate

of the particle-number operator

$$N = \sum_{jm} c^\dagger_{jm} c_{jm}. \tag{6}$$

Actually a nucleon-pair state $|jm, j-m\rangle$ is occupied with the probability of v_j^2 and empty with the probability u_j^2. The BCS ground state preserves, however, the particle-number parity indicating that the mixing happens only for states with an even number of particles. This is acceptable since the low-energy structure of nuclei shows certain independence of the particle number.

The BCS vacuum is not a particle vacuum but instead it is a vacuum state for a new kind of generalized annihilation operator a_{jm} obtained through the Bogoliubov-Valatin transformation [31, 32, 33]:

$$a_{jm} = u_j c_{jm} + v_j \tilde{c}^\dagger_{jm}. \tag{7}$$

Namely, the operator a_{jm} is a BCS quasiparticle annihilation operator and the corresponding BCS quasiparticle creation operator $a^\dagger_{jm}$ can be obtained through the hermitian conjugation. The BCS quasiparticles are fermions thus satisfying

$$\left\{a^\dagger_{j_1 m_1}, a_{j_2 m_2}\right\} = \delta_{j_1 j_2} \delta_{m_1 m_2}. \tag{8}$$

This condition is equivalent to a probability normalization of the amplitudes u_j and v_j:

$$u_j^2 + v_j^2 = 1. \tag{9}$$

Now the original mean-field Hamiltonian can be expressed in terms of the BCS quasiparticles. Including the ground state energy U_0, the expression turns out to have the structure

$$H = U_0 + H_{11} + H_{20} + H_{02} + \underbrace{H_{22} + H_{40} + H_{04} + H_{31} + H_{13}}_{V_{\mathrm{RES}}}, \tag{10}$$

where all the terms, except the ground state energy, are proportional to the normal ordered products of creation and annihilation operators:

$$H_{nk} \propto a^\dagger_{j_1 m_1} \ldots a^\dagger_{j_n m_n} a_{j'_1 m'_1} \ldots a_{j'_k m'_k}. \tag{11}$$

The occupation and unoccupation amplitudes, v_j and u_j, respectively, are determined by performing a constrained variation for the ground state energy. The variation is done for protons and neutrons separately and is constrained to yield a

given average value $\langle N \rangle$ of the proton or neutron number, equal to the actual value of the valence nucleons:

$$\frac{\partial}{\partial \langle N \rangle} \langle BCS | H - \lambda N | BCS \rangle = 0. \tag{12}$$

Here the Lagrange undetermined multiplier λ is chosen so that the particle number constraint is satisfied. Evaluating Eq. (12) reveals that most of the terms in the Hamiltonian H are trivial in the variational equation. In fact, only the static ground state energy term has a role in the treatment. The parameters u_j and v_j and physical quantities like the pairing gap and the quasiparticle energy can then be obtained by application of an iterative approach to the solution of the BCS equations.

Rewriting Eq. (12) indicates that λ is the chemical potential of the system:

$$\frac{\partial}{\partial \langle N \rangle} \langle BCS | H - \lambda N | BCS \rangle = 0 \;\; \Rightarrow \;\; \lambda = \frac{\partial}{\partial \langle N \rangle} \langle BCS | H | BCS \rangle. \tag{13}$$

This form shows that λ really is the rate at which the energy of the system is increasing when more particles are added to the system.

Besides minimizing the ground state energy, the BCS variational problem leads also to the vanishing of the terms H_{20} and H_{02} in (10). This property corresponds to the missing of the quasiparticle pair excitations across the Fermi surface but also shows how efficient the Bogoliubov-Valatin transformation (7) from the mean-field basis to the BCS basis is in absorbing part of the residual interaction to the structure of the quasiparticle ground state, $|BCS\rangle$.

2.3 The QRPA phonons

A good part of the interaction is already absorbed to the structure of the quasiparticles when making the transition from the independent particles to the BCS picture. Since quasiparticles are partly particles and partly holes the BCS ground state has a smooth Fermi surface instead of a sharp one as in the case of independent particles. Naturally most of the particles still occupy the lowest single-particle orbitals but there are some excitations present as well. Experimental data shows that this is not enough for the description of the ground state of an even-even nucleus and the quasiparticle correlations have to be included. Even though the BCS ground state is a quasiparticle vacuum, one has to allow the creation of quasiparticle pairs to the ground state by the residual interaction in order to describe collective states

in even-even nuclei. In the following a pair of quasiparticles on orbitals j_1 and j_2, coupled to angular momentum α_2 and its z-projection μ_2 is created by

$$\overline{A}^{\dagger}_{\alpha_2\mu_2}(j_1j_2) = \frac{\sqrt{1+\delta_{j_1j_2}(-1)^{\alpha_2}}}{1+\delta_{j_1j_2}}(a^{\dagger}_{j_1}a^{\dagger}_{j_2})_{\alpha_2\mu_2}, \tag{14}$$

where

$$(a^{\dagger}_{j_1}a^{\dagger}_{j_2})_{\alpha_2\mu_2} = \sum_{m_1m_2}\langle j_1m_1; j_2m_2|\alpha_2\mu_2\rangle a^{\dagger}_{j_1m_1}a^{\dagger}_{j_2m_2}. \tag{15}$$

A commonly used framework for introducing the quasiparticle-pair excitations in the ground state is the quasiparticle random-phase approximation, QRPA. The QRPA describes harmonic small-amplitude vibrations around a spherical nuclear shape [2, 3, 34] leading to collective low-energy solutions of the QRPA equations. The QRPA vacuum, $|QRPA\rangle$, is defined by

$$Q_{a_2\alpha_2\mu_2}|QRPA\rangle = 0, \tag{16}$$

where $Q_{a_2\alpha_2\mu_2}$ is the hermitian conjugate of the QRPA-phonon creation operator $Q^{\dagger}_{a_2\alpha_2\mu_2}$:

$$\begin{aligned} Q^{\dagger}_{a_2\alpha_2\mu_2} = \sum_{\tau=\pi,\nu}\sum_{j_1\le j_2}\Big[&X_{\tau}(j_1j_2;a_2\alpha_2)\overline{A}^{\dagger}_{\alpha_2\mu_2}(j_1j_2) \\ &- Y_{\tau}(j_1j_2;a_2\alpha_2)(-1)^{\alpha_2-\mu_2}\overline{A}_{\alpha_2-\mu_2}(j_1j_2)\Big]. \end{aligned} \tag{17}$$

The subscript $a_2\alpha_2\mu_2$ stands for the two-particle energy eigenvalue, angular momentum (and parity) and z-projection. In the sum over the quasiparticle states j_1 and j_2 a limited summation is used to avoid the same pairs to appear twice in the sum. The amplitudes $X_{\tau}(j_1j_2;a_2\alpha_2)$ and $Y_{\tau}(j_1j_2;a_2\alpha_2)$ are called the forward- and backward-going amplitudes, respectively. One should notice that the backward-going amplitude, $Y_{\tau}(j_1j_2;a_2\alpha_2)$, is a measure of the correlations in the ground state. Therefore, it is required that the amplitudes $Y_{\tau}(j_1j_2;a_2\alpha_2)$ remain small because otherwise the scheme of small vibrations will break down. This feature of the acceptable ground state can also be expressed by demanding the difference between the BCS and QRPA ground states to be small, i.e.,

$$|QRPA\rangle = |BCS\rangle + \text{small correlations}. \tag{18}$$

The QRPA problem can be formulated by using the equations of motion method, EOM, first introduced by Rowe [35]. The idea in the EOM is to reduce

the particle rank of the involved operators. This is done by using the symmetrized double commutators defined by

$$2[A,B,C]_{\pm} = [A,[B,C]]_{\pm} + [[A,B],C]_{\pm}, \tag{19}$$

where $+$ sign refers to fermionic operators (anticommutators) and $-$ sign to bosonic operators (commutators). In the EOM one of the operators in (19) is the nuclear Hamiltonian and one a given ansatz for the excitation operator of the theory, like the one of (17). Taking the vacuum expectation value of (19) makes the EOM exact for the true vacuum. The formalism also yields useful properties like the orthogonality and completeness for the resulting excitations. In the case of the QRPA, the EOM leads to the following double commutator equations:

$$\begin{aligned}\langle QRPA|\Big[\overline{A}_{\alpha_2\mu_2}(j_1j_2), H, Q^{\dagger}_{a_2\alpha_2\mu_2}\Big]|QRPA\rangle \\ = E_{a_2\alpha_2}\langle QRPA|\Big[\overline{A}_{\alpha_2\mu_2}(j_1j_2), Q^{\dagger}_{a_2\alpha_2\mu_2}\Big]|QRPA\rangle,\end{aligned} \tag{20}$$

$$\begin{aligned}\langle QRPA|\Big[\overline{A}^{\dagger}_{\alpha_2\mu_2}(j_1j_2), H, Q^{\dagger}_{a_2\alpha_2\mu_2}\Big]|QRPA\rangle \\ = E_{a_2\alpha_2}\langle QRPA|\Big[\overline{A}^{\dagger}_{\alpha_2\mu_2}(j_1j_2), Q^{\dagger}_{a_2\alpha_2\mu_2}\Big]|QRPA\rangle.\end{aligned} \tag{21}$$

To evaluate the involved commutators, the so called quasiboson approximation, QBA [36], is used. This way some terms in the commutators are omitted. In practice this leads to the replacement of the exact QRPA ground state by that of the BCS in the above equations. More explicitly, it causes the QRPA operators to fulfill the bosonic commutation rules:

$$\Big[Q_{a_2\alpha_2\mu_2}, Q^{\dagger}_{a_2'\alpha_2'\mu_2'}\Big] = \delta_{a_2a_2'}\delta_{\alpha_2\alpha_2'}\delta_{\mu_2\mu_2'}, \tag{22}$$

representing the expectation value of the commutator of two QRPA phonons with respect to the BCS vacuum. One should notice here that the BCS vacuum is not the exact vacuum of the QRPA and thus the derived QRPA equations are only approximative and are not based on a variational procedure.

The EOM equations (20) and (21) can be written as non-hermitian matrix equation

$$\begin{pmatrix} A & B \\ -B^* & -A^* \end{pmatrix}\begin{pmatrix} X_\tau \\ Y_\tau \end{pmatrix} = E_{a_2\alpha_2}\begin{pmatrix} X_\tau \\ Y_\tau \end{pmatrix}, \tag{23}$$

which is known as the QRPA matrix equation. Here $E_{a_2\alpha_2}$ is the QRPA eigenenergy and the corresponding eigenvector consists of all the amplitudes $X_\tau(j_1j_2;a_2\alpha_2)$ and $Y_\tau(j_1j_2;a_2\alpha_2)$. The submatrix $\mathbf{A}$ is hermitian and called the QTDA matrix because

it is the matrix to be solved in a more simple quasiparticle pair approach called the quasiparticle Tamm-Dancoff approximation [37, 38]. In the QTDA the ground state correlations are neglected completely. The other submatrix $\mathbf{B}$ is symmetric and can be called the correlation matrix. It appears due to the ground state correlations of the QRPA. Detailed expressions for the matrix elements of the A and B matrices are given in Ref. [39].

The QRPA eigenstates are obtained by diagonalizing the QRPA matrix (23). For these eigenstates the orthonormality (24) and completeness relations (25) and (26) are stated as

$$\sum_{\tau=\pi,\nu}\sum_{j_1\leq j_2}\Big[X_\tau(j_1j_2;a_2\alpha_2)^*X_\tau(j_1j_2;a_2'\alpha_2') - Y_\tau(j_1j_2;a_2\alpha_2)^*Y_\tau(j_1j_2;a_2'\alpha_2')\Big] = \delta_{a_2a_2'}\delta_{\alpha_2\alpha_2'}, \tag{24}$$

$$\sum_{\tau=\pi,\nu}\sum_{a_2}\Big[X_\tau(j_1j_2;a_2\alpha_2)X_\tau(j_1'j_2';a_2\alpha_2)^* - Y_\tau(j_1j_2;a_2\alpha_2)^*Y_\tau(j_1'j_2';a_2\alpha_2)\Big] = \delta_{j_1j_2}\delta_{j_1'j_2'}, \tag{25}$$

$$\sum_{\tau=\pi,\nu}\sum_{a_2}\Big[X_\tau(j_1j_2;a_2\alpha_2)Y_\tau(j_1'j_2';a_2\alpha_2)^* - Y_\tau(j_1j_2;a_2\alpha_2)^*X_\tau(j_1'j_2';a_2\alpha_2)\Big] = 0. \tag{26}$$

In completeness relations (25) and (26) it is required that $j_1 \leq j_2$ and $j_1' \leq j_2'$. Naturally, the dimension of the problem is twice as large as that of the corresponding QTDA problem and also the number of solutions is doubled when moving from the QTDA to QRPA. However, the number of the physical solutions in the QRPA remains the same as in the QTDA. This is due to the fact that to every physical solution with a positive eigenergy $E_{a_2\alpha_2}$ there is a negative eigenergy $E_{a_2'\alpha_2} = -E_{a_2\alpha_2}$. This negative-energy partner $E_{a_2'\alpha_2}$, $X_\tau(j_1j_2;a_2'\alpha_2)$, $Y_\tau(j_1j_2;a_2'\alpha_2)$ for the physical solution $E_{a_2\alpha_2}$, $X_\tau(j_1j_2;a_2\alpha_2)$, $Y_\tau(j_1j_2;a_2\alpha_2)$ can be obtained simply by setting $X_\tau(j_1j_2;a_2'\alpha_2) = Y_\tau(j_1j_2;a_2\alpha_2)^*$ and $Y_\tau(j_1j_2;a_2'\alpha_2) = X_\tau(j_1j_2;a_2\alpha_2)^*$.

2.4 Two-phonon like excitations

It is possible to extend the particle-hole basis by a direct inclusion of the 2p-2h terms within the extended QRPA [21] but the resulting equations are rather complicated.

In most applications it is preferred, for the sake of simplicity, to adopt the multistep technique in which building blocks are the QRPA phonons. These microscopic descriptions of multiphonon states and especially the double commutator technique to derive the EOM are actually particular realizations of the so called boson expansion technique [40]. This is also the way the two-phonon states of MAVA are built, i.e., in terms of QRPA degrees of freedom.

In the description of the low-lying excitations in even-even nuclei it is necessary to consider a general superposition of one- and two-phonon components leading to the excitation operator

$$\begin{aligned}\Gamma^{\dagger}_{a_4\alpha_4\mu_4} = &\sum_{a_2} Z_1(a_2;a_4\alpha_4)Q^{\dagger}_{a_2\alpha_4\mu_4} + \\ &\sum_{a_2\alpha_2\leq b_2\beta_2} Z_2(a_2\alpha_2 b_2\beta_2;a_4\alpha_4)(Q^{\dagger}_{a_2\alpha_2}Q^{\dagger}_{b_2\beta_2})_{\alpha_4\mu_4},\end{aligned} \tag{27}$$

where the two-particle quantum numbers, namely the energy eigenvalue, angular momentum and parity, are denoted by $(a_2\alpha_2)$. The quantum numbers $(a_4\alpha_4)$ denote the eigenvalue index and total spin-parity of the state with z-projection μ_4. The energies associated with these excitations are, of course, not just sums of the single-phonon energies. The eigenenergies and eigenstates can be found by using, for instance, the EOM technique, i.e.,

$$\left[H,\Gamma^{\dagger}_{a_4\alpha_4\mu_4}\right] = \mathcal{E}_{a_4\alpha_4}\Gamma^{\dagger}_{a_4\alpha_4\mu_4}, \tag{28}$$

where the Hamiltonian has the following phonon representation in terms of to the two-phonon basis

$$H = \sum_{c_2\gamma_2} E_{c_2\gamma_2}\sum_{\mu_2} Q^{\dagger}_{c_2\gamma_2\mu_2}Q_{c_2\gamma_2\mu_2}\ . \tag{29}$$

We can proceed in a similar way the QRPA equations were derived. Namely, the expectation value of the symmetrized double commutators between the Hamiltonian and the basis components entering (27) are computed using the BCS ground state as the approximative vacuum. After taking the vacuum expectation value of the involved commutators the following system of equations is obtained:

$$\begin{aligned}&\begin{pmatrix} E_{a_2\alpha_4}\delta_{a_2a_2'} & \mathcal{H}_{12}(a_2;a_2'\alpha_2'b_2'\beta_2') \\ \mathcal{H}_{21}(a_2\alpha_2b_2\beta_2;a_2') & \mathcal{H}_{22}(a_2\alpha_2b_2\beta_2;a_2'\alpha_2'b_2'\beta_2') \end{pmatrix}\begin{pmatrix} Z_1(a_2';a_4\alpha_4) \\ Z_2(a_2'\alpha_2'b_2'\beta_2';a_4\alpha_4)\end{pmatrix} \\ &= \mathcal{E}_{a4\alpha4}\begin{pmatrix} \delta_{a_2a_2'} & 0 \\ 0 & \mathcal{I}_{\alpha_4}(a_2\alpha_2b_2\beta_2;a_2'\alpha_2'b_2'\beta_2')\end{pmatrix}\begin{pmatrix} Z_1(a_2';a_4\alpha_4) \\ Z_2(a_2'\alpha_2'b_2'\beta_2';a_4\alpha_4)\end{pmatrix}.\end{aligned} \tag{30}$$

As defined earlier, $E_{a_2\alpha_2}$ denotes the QRPA eigenvalue, and $\mathcal{I}$ gives the overlap between the two-phonon states and is called the metric matrix.

In order to derive the metric matrix the exact commutators between two QRPA phonons are used instead of the bosonic commutation rule (22):

$$\begin{aligned}\left[Q_{a_2\alpha_2\mu_2}, Q^{\dagger}_{a_2'\alpha_2'\mu_2'}\right] = \delta_{a_2a_2'}\delta_{\alpha_2\alpha_2'}\delta_{\mu_2\mu_2'} + \sum_{\tau=\pi,\nu}\sum_{j_1j_2j_1'}\sum_{m_1m_2m_1'}\Big[\overline{X}_\tau(j_1j_2;a_2\alpha_2)\\ \times \overline{X}_\tau(j_1'j_1;a_2'\alpha_2')\langle j_1m_1;j_2m_2|\alpha_2\mu_2\rangle\langle j_1'm_1';j_1m_1|\alpha_2'\mu_2'\rangle\\ - \overline{Y}_\tau(j_1j_2;a_2\alpha_2)\overline{Y}_\tau(j_1'j_1;a_2'\alpha_2')\langle j_1m_1;j_2m_2|\alpha_2-\mu_2\rangle\\ \times \langle j_1'm_1';j_1m_1|\alpha_2'-\mu_2'\rangle(-1)^{\alpha_2+\alpha_2'-\mu_2-\mu_2'}\Big]a^{\dagger}_{j_1'm_1'}a_{j_2m_2}.\end{aligned} \tag{31}$$

The new amplitudes $\overline{X}_\tau(j_1j_2;a_2\alpha_2)$ are defined in terms of the old ones, the amplitudes of the restricted basis, as follows:

$$\overline{X}_\tau(j_1j_2;a_2\alpha_2) = \begin{cases} X_\tau(j_1j_2;a_2\alpha_2)\sqrt{1+\delta_{j_1j_2}(-1)^{\alpha_2}}, & j_1 \le j_2 \\ X_\tau(j_2j_1;a_2\alpha_2)\sqrt{1+\delta_{j_2j_1}(-1)^{\alpha_2}}(-1)^{j_1+j_2-\alpha_2+1}, & j_1 > j_2. \end{cases} \tag{32}$$

This leads to the unrestricted representation of the QRPA phonon which is simple to use in technical derivations. The metric matrix $\mathcal{I}$ of (30) takes into account the overcompleteness and non-orthogonality of the two-phonon basis and thus accounts for the Pauli principle:

$$\begin{aligned}\mathcal{I}_{\alpha_4}(a_2\alpha_2b_2\beta_2;a_2'\alpha_2'b_2'\beta_2') &= \langle 0|\Big[(Q_{b_2\beta_2}Q_{a_2\alpha_2})_{\alpha_4\mu_4},(Q^{\dagger}_{a_2'\alpha_2'}Q^{\dagger}_{b_2'\beta_2'})_{\alpha_4\mu_4}\Big]|0\rangle\\ &= \delta_{a_2a_2'}\delta_{\alpha_2\alpha_2'}\delta_{b_2b_2'}\delta_{\beta_2\beta_2'} + \delta_{a_2b_2'}\delta_{\alpha_2\beta_2'}\delta_{b_2a_2'}\delta_{\beta_2\alpha_2'}(-1)^{\alpha_2+\beta_2-\alpha_4}\\ &- \sum_{\tau=\pi,\nu}\sum_{j_1j_2j_3j_4}A^{(1)}_\tau(j_1j_2j_3j_4;a_2\alpha_2b_2\beta_2;a_2'\alpha_2'b_2'\beta_2'),\end{aligned} \tag{33}$$

where the matrix $A^{(1)}_\tau$ is given by

$$\begin{aligned}A^{(1)}_\tau(j_1j_2j_3j_4;a_2\alpha_2b_2\beta_2a_2'\alpha_2'b_2'\beta_2') \equiv \widehat{\alpha}_2\widehat{\beta}_2\widehat{\alpha}_2'\widehat{\beta}_2' \begin{Bmatrix} j_1 & j_2 & \alpha_2 \\ j_3 & j_4 & \beta_2 \\ \alpha_2' & \beta_2' & \alpha_4 \end{Bmatrix}\\ \times \Big[\overline{X}_\tau(j_1j_2;a_2\alpha_2)\overline{X}_\tau(j_3j_4;b_2\beta_2)\overline{X}_\tau(j_1j_3;a_2'\alpha_2')\overline{X}_\tau(j_2j_4;b_2'\beta_2')\\ - \overline{Y}_\tau(j_1j_2;a_2\alpha_2)\overline{Y}_\tau(j_3j_4;b_2\beta_2)\overline{Y}_\tau(j_1j_3;a_2'\alpha_2')\overline{Y}_\tau(j_2j_4;b_2'\beta_2')\Big].\end{aligned} \tag{34}$$

Above we have defined $\widehat{\alpha} = \sqrt{2\alpha+1}$. The second term in (34) contains the product of four Y_τ amplitudes and is therefore very small. This term can be safely neglected leading to the metric matrix with a TDA form, already used in Ref. [41].

The Hamiltonian matrix elements are given in terms of symmetrized double commutators. By using QRPA equation of motion (23) the elements $\mathcal{H}_{22}$ are found

to be proportional to the metric matrix, i.e.,

$$\begin{aligned}\mathcal{H}_{22}(a_2\alpha_2 b_2\beta_2; a_2'\alpha_2' b_2'\beta_2') &= \langle 0|\Big[(Q_{b_2\beta_2}Q_{a_2\alpha_2})_{\alpha_4\mu_4}, H, (Q^\dagger_{a_2'\alpha_2'}Q^\dagger_{b_2'\beta_2'})_{\alpha_4\mu_4}\Big]|0\rangle \\ &= \frac{1}{2}\Big[E_{a_2\alpha_2}+E_{b_2\beta_2}+E_{a_2'\alpha_2'}+E_{b_2'\beta_2'}\Big]\mathcal{I}_{\alpha_4}(a_2\alpha_2 b_2\beta_2; a_2'\alpha_2' b_2'\beta_2').\end{aligned} \tag{35}$$

The matrix element $\mathcal{H}_{22}$ gives the main contribution to the two-phonon energies as a sum of energies of its one-phonon constituents, corrected by the Pauli principle, thus having a clear physical meaning.

In order to derive the matrix elements connecting one-phonon with two-phonon components, the commutator of a QRPA phonon with the residual H_{31} interaction is considered. The residual interaction has the following form in the quasiparticle representation.

$$\begin{aligned}H_{31} = \sum_{\lambda_2\mu_2}\sum_{\tau=\pi,\nu}\sum_{j_1j_2j_3j_4} & V^{(31)}_{j_1j_2j_3j_4}(\tau\lambda_2)(-1)^{\lambda_2-\mu_2} \\ & \times\Big[(a^\dagger_{j_1}a^\dagger_{j_2})_{\lambda_2\mu_2}(a^\dagger_{j_3}\tilde{a}_{j_4})_{\lambda_2-\mu_2}+H.c.\Big],\end{aligned} \tag{36}$$

where the isospin indices are dropped out except under the summation sign. Here the conventional abbreviation $V^{(31)}_{j_1j_2j_3j_4}(\tau\lambda_2)$ includes the two-body matrix element $\langle\tau j_1\tau j_2;\lambda_2|V|\tau j_3\tau j_4;\lambda_2\rangle$ with the two-body interaction V

$$\begin{aligned}V^{(31)}_{j_1j_2j_3j_4}(\tau\lambda_2) =& -\frac{1}{2}\sqrt{1+\delta_{j_1j_2}(-1)^{\lambda_2}}\sqrt{1+\delta_{j_3j_4}(-1)^{\lambda_2}} \\ & \times(u_{j_1}u_{j_2}v_{j_3}u_{j_4}-v_{j_1}v_{j_2}u_{j_3}v_{j_4})\langle\tau j_1\tau j_2;\lambda_2|V|\tau j_3\tau j_4;\lambda_2\rangle \\ =&(u_{j_1}u_{j_2}v_{j_3}u_{j_4}-v_{j_1}v_{j_2}u_{j_3}v_{j_4})G(j_1j_2j_3j_4\lambda_2).\end{aligned} \tag{37}$$

The notation $G(j_1j_2j_3j_4\lambda_2)$ is commonly used and is originally introduced by Baranger [34]. The commutator of a QRPA phonon with the residual H_{31} interaction can be

cast into a form written in terms of two QRPA phonons, i.e.,

$$
\begin{aligned}
\Big[H_{31},Q^{\dagger}_{a_2\alpha_4\mu_4}\Big] &= \sum_{d_2\delta_2c_2\gamma_2}\sum_{\lambda_2}\sum_{\tau=\pi,\nu}\sum_{j_1j_2j_3j_4}V^{(31)}_{j_1j_2j_3j_4}(\tau\lambda_2)\sum_{j\le j'}\overline{X}_{\tau}(jj';a_2\alpha_4)\\
&\times\frac{\sqrt{1+\delta_{jj'}(-1)^{\alpha_4}}}{1+\delta_{jj'}}\Bigg(\delta_{\delta_2\lambda_2}\widehat{\lambda}_2\widehat{\gamma}_2\Big\{\overline{X}_{\tau}(j_1j_2;d_2\lambda_2)\Big[x_{\tau}(\lambda_2j_3\alpha_4j';j\gamma_2;c_2)\delta_{j_4j}\\
&-(-1)^{j+j_4-\alpha_4}x_{\tau}(\lambda_2j_3\alpha_4j;j'\gamma_2;c_2)\delta_{j_4j'}\Big]\\
&+(-1)^{j_4-j_3+\lambda_2}\overline{Y}_{\tau}(j_1j_2;d_2\lambda_2)\Big[x_{\tau}(\lambda_2j_4\alpha_4j';j\gamma_2;c_2)\delta_{j_3j}\\
&-(-1)^{j+j_3-\alpha_4}x_{\tau}(\lambda_2j_4\alpha_4j:j'\gamma_2;c_2)\delta_{j_3j'}\Big]\Big\}\\
&+(\widehat{\lambda}_2)^2\widehat{\gamma}_2\widehat{\delta}_2(-1)^{\delta_2}\Big\{(-1)^{j_2+j_3}y_{\tau}(j_4j_3j_1j_2;\lambda_2\gamma_2;c_2)\\
&\times\Big[(-1)^{j_1+j}x_{\tau}(\gamma_2j_4\alpha_4j;j'\delta_2;d_2)\delta_{j_1j'}-(-1)^{\alpha_4}x_{\tau}(\gamma_2j_4\alpha_4j';j\delta_2;d_2)\delta_{j_1j}\Big]\\
&-(-1)^{\lambda_2-\alpha_4}y_{\tau}(j_4j_3j_2j_1;\lambda_2\gamma_2;c_2)\Big[(-1)^{j_3+j}x_{\tau}(\gamma_2j_4\alpha_4j;j'\delta_2;d_2)\delta_{j_2j'}\\
&+(-1)^{j_2+j_3}x_{\tau}(\gamma_2j_4\alpha_4j';j\delta_2;d_2)\delta_{j_2j}\Big]\Big\}\Bigg)(Q^{\dagger}_{d_2\delta_2}Q^{\dagger}_{c_2\gamma_2})_{\alpha_4\mu_4}\\
&=\sum_{d_2\delta_2c_2\gamma_2}C(d_2\delta_2c_2\gamma_2;a_2\alpha_4)(Q^{\dagger}_{d_2\delta_2}Q^{\dagger}_{c_2\gamma_2})_{\alpha_4\mu_4}.
\end{aligned}
\tag{38}
$$

Again the isospin indices are dropped except under the summation sign and in the amplitudes and the following notations are introduced:

$$x_{\tau}(\lambda_2j_3\alpha_4j';j\gamma_2;c_2) = W(\lambda_2j_3\alpha_4j';j\gamma_2)\overline{X}_{\tau}(j_3j';c_2\gamma_2), \tag{39}$$

$$y_{\tau}(j_4j_3j_1j_2;\lambda_2\gamma_2;c_2) = W(j_4j_3j_1j_2;\lambda_2\gamma_2)\overline{Y}_{\tau}(j_2j_3;c_2\gamma_2), \tag{40}$$

where $W(abcd;ef)$ denotes the Racah coefficient [42].

In deriving Eq. (38) the $Y_{\tau}Y_{\tau}$ products are neglected for simplicity since they are small. Now the rest of the Hamiltonian matrix elements can be written as

$$
\begin{aligned}
\mathcal{H}_{21}(a_2\alpha_2b_2\beta_2;a_2') &= \langle 0|\Big[(Q_{b_2\beta_2}Q_{a_2\alpha_2})_{\alpha_4\mu_4},H,Q^{\dagger}_{a_2'\alpha_4\mu_4}\Big]|0\rangle\\
&=\frac{1}{2}\sum_{d_2\delta_2c_2\gamma_2}C(d_2\delta_2c_2\gamma_2;a_2'\alpha_4)\mathcal{I}_{\alpha_4}(a_2\alpha_2b_2\beta_2;d_2\delta_2c_2\gamma_2),
\end{aligned}
\tag{41}
$$

$$
\begin{aligned}
\mathcal{H}_{12}(a_2;a_2'\alpha_2'b_2'\beta_2') &= \langle 0|\Big[Q_{a_2\alpha_4\mu_4},H,(Q^{\dagger}_{a_2'\alpha_2'}Q^{\dagger}_{b_2'\beta_2'})_{\alpha_4\mu_4}\Big]|0\rangle\\
&=\frac{1}{2}\sum_{d_2\delta_2c_2\gamma_2}C(d_2\delta_2c_2\gamma_2;a_2\alpha_4)\mathcal{I}_{\alpha_4}(d_2\delta_2c_2\gamma_2;a_2'\alpha_2'b_2'\beta_2')\\
&=\mathcal{H}_{21}(a_2'\alpha_2'b_2'\beta_2';a_2).
\end{aligned}
\tag{42}
$$

A similar procedure to estimate the coupling between the one- and two-phonon basis components is used in the quasiparticle-phonon model (QPM) [13].

In order to solve the eigenvalue system of equations (30) for the general wave function (27) the standard technique is used [41]. One should notice that the metric matrix is not diagonal since the initial basis is not orthogonal. The orthonormal basis is built by first diagonalizing the metric matrix and using the resulting eigenstates as new basis. The original basis is also overcomplete containing spurious basis vectors. The spurious basis states correspond to very small eigenvalues of the metric matrix and they can be thus eliminated. The new orthogonal, complete basis leads to a system of equations of the standard Hermitian form.

2.4.1 MAVA2

In this subsection the relations improving the MAVA formalism are presented. The enhanced version is called MAVA2 and it has been used in **PIII**. The improvement is done by a proper consideration of the fermionic structure of the QRPA phonons, i.e., now we go beyond the quasiboson approximation [43] in the commutators. Refinement of the expression (35) is obtained by considering the exact double commutation relation (19) between the QRPA phonons and the Hamiltonian. The resulting expression reads

$$
\begin{aligned}
\mathcal{H}_{22}(a_2\alpha_2 b_2\beta_2; a_2'\alpha_2' b_2'\beta_2') &= \langle 0|\Big[(Q_{b_2\beta_2}Q_{a_2\alpha_2})_{\alpha_4\mu_4}, H, (Q^\dagger_{a_2'\alpha_2'}Q^\dagger_{b_2'\beta_2'})_{\alpha_4\mu_4}\Big]|0\rangle \\
&= \frac{1}{2}\Big[E_{a_2\alpha_2}+E_{b_2\beta_2}+E_{a_2'\alpha_2'}+E_{b_2'\beta_2'}\Big]\mathcal{I}_{\alpha_4}(a_2\alpha_2 b_2\beta_2; a_2'\alpha_2' b_2'\beta_2') \\
&- \frac{1}{2}\Big\{\Big[E_{a_2\alpha_2}+E_{a_2'\alpha_2'}\Big]\langle 0|Q_{b_2\beta_2}N_{a_2\alpha_2;a_2'\alpha_2'}Q^\dagger_{b_2'\beta_2'}|0\rangle_{\alpha_4\mu_4} \\
&+ E_{b_2\beta_2}(-1)^{\alpha_2+\beta_2-\alpha_4}\langle 0|Q_{a_2\alpha_2}N_{b_2\beta_2;a_2'\alpha_2'}Q^\dagger_{b_2'\beta_2'}|0\rangle_{\alpha_4\mu_4} \\
&+ E_{b_2'\beta_2'}(-1)^{\alpha_2'+\beta_2'-\alpha_4}\langle 0|Q_{b_2\beta_2}N_{a_2\alpha_2;b_2'\beta_2'}Q^\dagger_{a_2'\alpha_2'}|0\rangle_{\alpha_4\mu_4}\Big\} \\
&+ \sum_{c_2\gamma_2} E_{c_2\gamma_2}\langle 0|Q_{b_2\beta_2}N_{a_2\alpha_2;c_2\gamma_2}N_{c_2\gamma_2;a_2'\alpha_2'}Q^\dagger_{b_2'\beta_2'}|0\rangle_{\alpha_4\mu_4} \\
&= \frac{1}{2}\Big[E_{a_2\alpha_2}+E_{b_2\beta_2}+E_{a_2'\alpha_2'}+E_{b_2'\beta_2'}\Big] \\
&\times\Big\{\mathcal{I}_{\alpha_4}(a_2\alpha_2 b_2\beta_2; a_2'\alpha_2' b_2'\beta_2') - \langle 0|Q_{b_2\beta_2}N_{a_2\alpha_2;a_2'\alpha_2'}Q^\dagger_{b_2'\beta_2'}|0\rangle_{\alpha_4\mu_4}\Big\} \\
&+ \sum_{c_2\gamma_2} E_{c_2\gamma_2}\langle 0|Q_{b_2\beta_2}N_{a_2\alpha_2;c_2\gamma_2}N_{c_2\gamma_2;a_2'\alpha_2'}Q^\dagger_{b_2'\beta_2'}|0\rangle_{\alpha_4\mu_4},
\end{aligned}
\tag{43}
$$

where the $N_{a_2\alpha_2\mu_2;a_2'\alpha_2'\mu_2'}$ matrices contain information beyond the quasiboson approximation, i.e., they include the exact commutator between two QRPA phonons

as defined in (31). Rewriting Eq. (31) as

$$\left[Q_{a_2\alpha_2\mu_2}, Q^{\dagger}_{a_2'\alpha_2'\mu_2'}\right] = \delta_{a_2a_2'}\delta_{\alpha_2\alpha_2'}\delta_{\mu_2\mu_2'} + N_{a_2\alpha_2\mu_2;a_2'\alpha_2'\mu_2'} \tag{44}$$

the explicit form of the $N_{a_2\alpha_2\mu_2;a_2'\alpha_2'\mu_2'}$ matrix is found to be

$$\begin{aligned} N_{a_2\alpha_2\mu_2;a_2'\alpha_2'\mu_2'} \approx \sum_{\tau=\pi,\nu}\sum_{j_1j_2j_1'}\sum_{m_1m_2m_1'} & \Big[\overline{X}_\tau(j_1j_2;a_2\alpha_2)\overline{X}_\tau(j_1'j_1;a_2'\alpha_2') \\ & \times \langle j_1m_1;j_2m_2|\alpha_2\mu_2\rangle\langle j_1'm_1';j_1m_1|\alpha_2'\mu_2'\rangle\Big] a^{\dagger}_{j_1'm_1'}a_{j_2m_2}. \end{aligned} \tag{45}$$

The approximation is coming from the fact that terms containing $Y_\tau Y_\tau$ products are neglected. The expectation value of the $N_{a_2\alpha_2;a_2'\alpha_2'}$ operator is written as

$$\begin{aligned} \langle 0|Q_{b_2\beta_2}N_{a_2\alpha_2;a_2'\alpha_2'}Q^{\dagger}_{b_2'\beta_2'}|0\rangle_{\alpha_4\mu_4} &\equiv \sum_{\mu_2\nu_2}\sum_{\mu_2'\nu_2'}\langle\alpha_2\mu_2;\beta_2\nu_2|\alpha_4\mu_4\rangle\langle\alpha_2'\mu_2';\beta_2'\nu_2'|\alpha_4\mu_4\rangle \\ &\times\langle 0|Q_{b_2\beta_2\nu_2}N_{a_2\alpha_2\mu_2;a_2'\alpha_2'\mu_2'}Q^{\dagger}_{b_2\beta_2'\nu_2'}|0\rangle \\ &\approx \sum_{\tau=\pi,\nu}\sum_{j_1j_2j_3j_4}A^{(1)}_\tau(j_1j_2j_3j_4;a_2\alpha_2b_2\beta_2a_2'\alpha_2'b_2\beta_2') \\ &= (-1)^{\alpha_2+\beta_2+\alpha_4}\langle 0|Q_{a_2\alpha_2}N_{b_2\beta_2;a_2'\alpha_2'}Q^{\dagger}_{b_2'\beta_2'}|0\rangle_{\alpha_4\mu_4} \\ &= (-1)^{\alpha_2'+\beta_2'+\alpha_4}\langle 0|Q_{b_2\beta_2}N_{a_2\alpha_2;b_2'\beta_2'}Q^{\dagger}_{a_2'\alpha_2'}|0\rangle_{\alpha_4\mu_4}\ . \end{aligned} \tag{46}$$

Again $Y_\tau Y_\tau$ and $Y_\tau Y_\tau Y_\tau Y_\tau$ QRPA amplitudes are neglected and Eq. (34) gives the definition for the shorthand notation $A^{(1)}_\tau(j_1j_2j_3j_4;a_2\alpha_2b_2\beta_2a_2'\alpha_2'b_2'\beta_2')$. The second needed expectation value is of the $N_{a_2\alpha_2;c_2\gamma_2}N_{c_2\gamma_2;a_2'\alpha_2'}$ operator

$$\begin{aligned} \langle 0|Q_{b_2\beta_2}N_{a_2\alpha_2;c_2\gamma_2}N_{c_2\gamma_2;a_2'\alpha_2'}Q^{\dagger}_{b_2'\beta_2'}|0\rangle_{\alpha_4\mu_4} &\equiv \sum_{\xi_2\mu_2\nu_2}\sum_{\mu_2'\nu_2'}\langle\alpha_2\mu_2;\beta_2\nu_2|\alpha_4\mu_4\rangle \\ &\times\langle\alpha_2'\mu_2';\beta_2'\nu_2'|\alpha_4\mu_4\rangle\langle 0|Q_{b_2\beta_2\nu_2}N_{a_2\alpha_2\mu_2;c_2\gamma_2\xi_2}N_{c_2\gamma_2\xi_2;a_2'\alpha_2'\mu_2'}Q^{\dagger}_{b_2'\beta_2'\nu_2'}|0\rangle \\ &\approx \sum_{\tau=\pi,\nu}\sum_{j_1j_2j_3j_4}\sum_{jj'}\sum_{\delta_2}A^{(2)}_\tau(j_1j_2j_3j_4jj';a_2\alpha_2b_2\beta_2a_2'\alpha_2'B_2'\beta_2'c_2\gamma_2d_2\delta_2)\ , \end{aligned} \tag{47}$$

where

$$
\begin{aligned}
&A^{(2)}_{\tau}(j_1j_2j_3j_4jj';a_2\alpha_2b_2\beta_2a'_2\alpha'_2b'_2\beta'_2c_2\gamma_2d_2\delta_2) \equiv \widehat{\alpha}_2\widehat{\beta}_2\widehat{\gamma}_2\widehat{\delta}_2 \left\{ \begin{array}{ccc} j_1 & j_2 & \alpha_2 \\ j_3 & j_4 & \beta_2 \\ \gamma_2 & \delta_2 & \alpha_4 \end{array} \right\} \\
&\times \overline{X}_{\tau}(j_1j_2;a_2\alpha_2)\overline{X}_{\tau}(j_3j_4;b_2\beta_2)\widehat{\alpha}'_2\widehat{\beta}'_2\widehat{\gamma}_2\widehat{\delta}_2 \Bigg[\left\{ \begin{array}{ccc} j & j_2 & \alpha'_2 \\ j' & j_4 & \beta'_2 \\ \gamma_2 & \delta_2 & \alpha_4 \end{array} \right\} \\
&\times \overline{X}_{\tau}(jj_2;a'_2\alpha'_2)\overline{X}_{\tau}(j'j_4;b'_2\beta'_2) - (-1)^{j_2+j_4+\delta_2} \left\{ \begin{array}{ccc} j & j_4 & \alpha'_2 \\ j' & j_2 & \beta'_2 \\ \gamma_2 & \delta_2 & \alpha_4 \end{array} \right\} \\
&\times \overline{X}_{\tau}(jj_4;a'_2\alpha'_2)\overline{X}_{\tau}(j'j_2;b'_2\beta'_2) \Bigg] \overline{X}_{\tau}(j_1j_3;c_2\gamma_2)\overline{X}_{\tau}(jj';c_2\gamma_2) \\
&\equiv a^{(1)}_{\tau}(j_1j_2j_3j_4;a_2\alpha_2b_2\beta_2c_2\gamma_2d_2\delta_2) \Big[a^{(1)}_{\tau}(jj_2j'j_4;a'_2\alpha'_2b'_2\beta'_2c_2\gamma_2d_2\delta_2) \\
&- (-1)^{j_2+j_4+\delta_2} a^{(1)}_{\tau}(jj_4j'j_2;a'_2\alpha'_2b_2\beta'_2c_2\gamma_2d_2\delta_2) \Big] \overline{X}_{\tau}(j_1j_3;c_2\gamma_2)\overline{X}_{\tau}(jj';c_2\gamma_2) \ .
\end{aligned}
\tag{48}
$$

Here it is worth mentioning that besides corrections coming from the Pauli principle and orthonormalization, i.e., the $N_{a_2\alpha_2\mu_2;a'_2\alpha'_2\mu'_2}$ matrices, the two-phonon states do not interact via additional two-body interactions. Taking into account the direct two-phonon-two-phonon interaction usually gives rise to additional anharmonicities, thus being a matter whose importance should be studied in the future.

3 ELECTROMAGNETIC INTERACTION

The electromagnetic interaction allows the nucleus to make transitions between its states by exchanging photons with its surroundings. Thus the study of nuclear decay rates via gamma decays is a good test of the nuclear wave functions obtained in a nuclear model. Moreover, nuclear gamma-decay properties are some of the best indicators of nuclear spin and parity J^π of excited states. In the next section the basic concepts related to electromagnetic transitions in nuclei are described and, moreover, the needed matrix elements are given in the framework of MAVA.

3.1 General

When going from an initial state $|\Psi_i\rangle$ to a final state $|\Psi_f\rangle$ of a nucleus by emitting or absorbing electromagnetic radiation of multipolarity J, the transition probability per unit time can be compactly written as

$$T_{fi}^{(JM)} = \frac{2(J+1)}{\epsilon_0 \hbar J[(2J+1)!!]^2} \left(\frac{E_\gamma}{\hbar c}\right)^{2J+1} |\langle \xi_f J_f M_f | T_{JM} | \xi_i J_i M_i \rangle|^2. \quad (49)$$

Here the operator T_{JM} is either an electric or magnetic multipole operator, with multipolarity JM, and E_γ is the energy of the transition. The total transition probability can be obtained by performing summation over the magnetic quantum numbers:

$$T_{fi}^{(J)} \equiv \frac{1}{2J_i+1} \sum_{M M_i M_f} T_{fi}^{(JM)} = \frac{2(J+1)}{\epsilon_0 \hbar J[(2J+1)!!]^2} \left(\frac{E_\gamma}{\hbar c}\right)^{2J+1} B(J; J_i \to J_f), \quad (50)$$

where the reduced transition probability $B(EJ)$ (electric) and $B(MJ)$ (magnetic) have the forms

$$B(EJ; J_i \to J_f) \equiv \frac{1}{2J_i+1} \left|(\xi_f J_f||Q_J||\xi_i J_i)\right|^2, \tag{51}$$

$$B(MJ; J_i \to J_f) \equiv \frac{1}{2J_i+1} \left|(\xi_f J_f||M_J||\xi_i J_i)\right|^2. \tag{52}$$

Above the electric and magnetic operators are given in the SI units as

$$Q_{JM} = \xi^{(EJ)} \sum_{i=1}^{A} e_\tau(i) r_i^J Y_{JM}(\Omega_i), \tag{53}$$

$$M_{JM} = \frac{\mu_N}{\hbar c} \xi^{(MJ)} \sum_{i=1}^{A} \left[g_{s(i)}^{(\tau)} \mathrm{s}(i) + \frac{2}{J+1} g_{l(i)}^{(\tau)} \mathrm{l}(i) \right] \cdot \nabla_i [r_i^J Y_{JM}(\Omega_i)]. \tag{54}$$

Here e_τ is the electric charge of proton or neutron, bare values being unit of charge for protons and zero for neutrons. The g-factors, or gyromagnetic ratios, $g_s^{(\tau)}$ and $g_l^{(\tau)}$, as well as the phase factors $\xi^{(EJ)}$ and $\xi^{(MJ)}$ can be found e.g., from Ref. [43]. The nuclear magneton includes the proton mass m_p and has the following expression

$$\mu_N = \frac{e\hbar}{2m_p} \simeq 0.105 ce\text{fm}. \tag{55}$$

3.2 Electric transitions in the MAVA scheme

The electric transitions between states containing only two-phonon components were described in Ref. [44]. Here a more general case related to the wave function (27) is considered. Starting with a spherical tensor of rank J, in this case the electric operator of multipolarity J (53), one can write in second quantization as follows:

$$\begin{aligned} Q_{JM} &= \sum_{\tau=\pi,\nu} \sum_{j_1 j_2} \sum_{m_1 m_2} \langle \tau j_1 m_1 | Q_{JM} | \tau j_2 m_2 \rangle c^\dagger_{j_1 m_1} c_{j_2 j m_2} \\ &= \frac{1}{\hat{J}} \sum_{\tau=\pi,\nu} \sum_{j_1 j_2} \langle \tau j_1 || Q_J || \tau j_2 \rangle (c^\dagger_{j_1} \tilde{c}_{j_2})_{JM}. \end{aligned} \tag{56}$$

Expressing then $(c^\dagger_{j_1} \tilde{c}_{j_2})_{JM}$ in terms of quasiparticle operators gives

$$\begin{aligned} (c^\dagger_{j_1} \tilde{c}_{j_2})_{JM} = {} & u_{j_1} u_{j_2} (a^\dagger_{j_1} \tilde{a}_{j_2})_{JM} + u_{j_1} v_{j_2} (a^\dagger_{j_1} a^\dagger_{j_2})_{JM} \\ & - v_{j_1} u_{j_2} (\tilde{a}_{j_1} \tilde{a}_{j_2})_{JM} - v_{j_1} v_{j_2} (\tilde{a}_{j_1} a^\dagger_{j_2})_{JM}. \end{aligned} \tag{57}$$

In the used method the scattering terms $a^{\dagger}\tilde{a}$ are neglected to first approximation leading to the following representation of the particle-hole part of the transition operator, consistent with the QRPA phonon

$$Q_{JM} = \sum_{\tau=\pi,\nu} \sum_{j_1 \leq j_2} \xi_{\tau J}(j_1 j_2) \Big[\overline{A}^{\dagger}_{JM}(j_1 j_2) + (-1)^{J-M} \overline{A}_{J-M}(j_1 j_2) \Big], \tag{58}$$

where

$$\xi_{\tau J}(j_1 j_2) = \frac{\sqrt{1+\delta_{j_1 j_2}(-1)^J}}{\widehat{J}(1+\delta_{j_1 j_2})} \langle \tau j_1 || Q_J || \tau j_2 \rangle (u_{j_1} v_{j_2} + v_{j_1} u_{j_2}). \tag{59}$$

The reduced matrix element connecting a MAVA eigenstate with the ground state is given in terms of the one-phonon amplitudes of the operator (27), i.e.,

$$\begin{aligned} \langle a_4 \alpha_4 || Q_{\alpha_4} || 0 \rangle = \widehat{\alpha}_4 \sum_{a_2} Z_1(a_2; a_4 \alpha_4) \\ \times \sum_{\tau=\pi,\nu} \sum_{j_1 \leq j_2} \xi_{\tau \alpha_4}(j_1 j_2) \Big[X_{\tau}(j_1 j_2; a_2 \alpha_4) + Y_{\tau}(j_1 j_2; a_2 \alpha_4) \Big]. \end{aligned} \tag{60}$$

The transition amplitude between two MAVA eigenstates is given by the superposition of components containing products between the one- and two-phonon amplitudes, multiplied by the metric matrix:

$$\begin{aligned} \langle a'_4 \alpha'_4 || Q_{\gamma_2} || a_4 \alpha_4 \rangle = \sum_{\tau=\pi,\nu} \sum_{j_1 \leq j_2} \sum_{c_2} \xi_{\tau \gamma_2}(j_1 j_2) \Big[X_{\tau}(j_1 j_2; c_2 \gamma_2) + Y_{\tau}(j_1 j_2; c_2 \gamma_2) \Big] \\ \times \Big\{ \widehat{\alpha}'_4 \sum_{a_2} \sum_{a'_2 \alpha'_2 \leq b'_2 \beta'_2} Z_1(a_2; a_4 \alpha_4) Z_2(a'_2 \alpha'_2 b'_2 \beta'_2; a'_4 \alpha'_4) \mathcal{I}_{\alpha'_4}(a'_2 \alpha'_2 b'_2 \beta'_2; a_2 \alpha_4 c_2 \gamma_2) \\ + \widehat{\alpha}_4 \sum_{a'_2} \sum_{a_2 \alpha_2 \leq b_2 \beta_2} Z_1(a'_2; a'_4 \alpha'_4) Z_2(a_2 \alpha_2 b_2 \beta_2; a_4 \alpha_4) \mathcal{I}_{\alpha_4}(a'_2 \alpha'_4 c_2 \gamma_2; a_2 \alpha_2 b_2 \beta_2) \Big\}. \end{aligned} \tag{61}$$

Eqs. (30) and (61) now testify that the metric matrix, taking into consideration the Pauli principle, is crucial in describing both eigenstates and electromagnetic transitions within the MAVA scheme.

4 NUCLEAR-STRUCTURE CALCULATIONS

The performed nuclear-structure calculations for cadmium, ruthenium and molybdenum isotopes will be described in this section. The treatment is based on the theoretical framework outlined in the previous sections. First, the construction of the quasiparticle basis is discussed, and after that, the description of the QRPA calculations follows. Finally, the MAVA calculations and their results are reviewed.

4.1 Single-particle basis

To set up the calculations a set of single-particle states, the valence space, is chosen. The method applied, when selecting this set of active single-particle orbitals, was to include all the levels within a sufficiently large range below and above the Fermi surface. The sufficiency is determined by the requirement to be able to handle all the low-energy phenomena within the chosen valence space. In practice, it is convenient to restrict oneself to a few harmonic-oscillator major shells, not forgetting the possible intruding states from the higher shells. The chosen basis consists of ten proton and neutron single-particle levels around the proton and neutron Fermi surfaces, spanning the valence space: $1p0f - 2s1d0g - 0h_{11/2}$ for the studied molybdenum and ruthenium isotopes. For the studied cadmium isotopes the above mentioned valence space is chosen for protons and a rather large basis of 15 neutron single-particle levels consisting of the $1p0f - 2s1d0g - 2p1f0h$ shells for the neutrons.

The single-particle energies of the orbitals were calculated by using the phe-

nomenological, Bohr-Mottelson [24] parametrized, Woods-Saxon potential. In addition to the radial Woods-Saxon and kinetic parts, this single-particle potential contains the centrifugal term, the spin-orbit coupling, and, in the case of protons, the Coulomb potential of a uniformly charged sphere. The single-particle wave functions are, however, taken to be the eigenstates of a spherical harmonic-oscillator with a suitable oscillator constant. This is a good approximation for bound states in nuclei [43].

The two-body interaction, corresponding to H_{RES} in Eq. (4), was taken to be the G matrix generated from the Bonn one-boson-exchange potential [45] as done in [46]. The different channels of this interaction are scaled by constants as described in Refs. [47, 48]. The interaction matrix elements were scaled within the BCS and QRPA calculations in order to take into account the renormalization due to the limited size of the valence space.

4.2 BCS calculations

The construction of the quasiparticle basis was done by performing a BCS calculation for all the studied nuclei. The amplitudes u and v, introduced in the definition of the BCS ground state (5), and the quasiparticle energies were found as a result of the minimization of the BCS ground state energy.

The quasiparticle structure depends on the two-body interaction via the monopole matrix elements of the form

$$g^{pair}\langle j_1 j_1; J=0|H_{\mathrm{RES}}|j_2 j_2; J=0\rangle, \tag{62}$$

where g^{pair} is the pairing-strength parameter fixed for the protons and neutrons separately. The adjustment of the pairing strength parameter is based on the use of a phenomenological pairing-gap formula, giving the pairing-induced odd-even staggering of the nuclear masses in terms of the proton and neutron separation energies [49], S_p and S_n, respectively. Accordingly, the pairing gaps for protons and neutrons read

$$\Delta_p({}^{A}_{Z}X_N) = -\frac{1}{4}\left[S_p({}^{A+1}_{Z+1}X_N) - 2S_p({}^{A}_{Z}X_N) + S_p({}^{A-1}_{Z-1}X_N)\right], \tag{63}$$

$$\Delta_n({}^{A}_{Z}X_N) = -\frac{1}{4}\left[S_n({}^{A+1}_{Z}X_{N+1}) - 2S_n({}^{A}_{Z}X_N) + S_n({}^{A-1}_{Z}X_{N-1})\right], \tag{64}$$

where ${}^{A}_{Z}X_{N}$ stands for the doubly-even nucleus for which the BCS calculation is being done. According to the BCS approach this pairing gap is equal to the lowest quasiparticle energy. Hence, the pairing strength was adjusted in such a way that the experimental pairing gap was reproduced. The required renormalization was rather modest, generally g^{pair} was in the range of 0.88-1.18.

The quasiparticle spectrum provides a way to infer if the Woods-Saxon energies reflect the actual single-particle values. This arises from the assumption of a dominant one quasiparticle structure of the few lowest-energy states of an odd-mass nucleus. If the quasiparticle spectrum looks very different from the experimental low-energy spectrum of the neighbouring odd-mass nucleus, then some modifications of the single-particle energies are needed. In practice, one makes minor changes to the Woods-Saxon energies near the Fermi surface, always preserving the right ordering of the spin-orbit partners. Generally, the effect of altering the single-particle energy can be summarized as follows: the closer to the Fermi surface a level is brought, the lower the quasiparticle energy will be, and vice versa. Changing the energy of some of the levels can produce, however, more complicated changes in the overall quasiparticle spectrum. In the following calculations the single-particle energies obtained by using the Woods-Saxon potential were used without any modifications.

4.3 QRPA calculations

Once the quasiparticle basis has constructed by the BCS method, the QRPA calculations could be done to obtain the ground state and the excitations of the doubly-even nuclei. Also the QRPA includes a way to renormalize the interaction . The parameters g_{ph} and g_{pp} represent the scaling of the particle-hole and particle-particle modes of interaction, respectively. In the present work, the parameters were adjusted for the 2^+ and 4^+ states, aiming to match the lowest QRPA energy and the corresponding experimental value in each case. If the experimental value was out of reach using a reasonable tuning of the interaction, the parameter was taken to be 1.0, suggesting the possibility that the experimental state could have a more complicated structure than the one-phonon QRPA state (17). Generally, the one-phonon states were easy to recognize in the experimental spectrum. In particular, when studying 4^+ states, one should note that the two-phonon triplet corresponding to the $2^+_1 \otimes 2^+_1$ coupling, which we are interested in, are not described by the QRPA.

This is because QRPA deals with two-quasiparticle excitations only and thus the g_{ph} parameter for 4^+ states should be adjusted so that the energy of the second lowest of the experimental states is correctly reproduced.

4.4 MAVA calculations

The metric matrix, consisting of overlaps between all the two-phonon combinations included in the calculations, is contained as a relevant part in the MAVA formalism. The angular-momentum dependence of the metric matrix contributes to the splitting of the two-phonon-like MAVA states. The Pauli principle is preserved in diagonalization of the metric matrix as described in detail in [50]. It should be mentioned that the results for the calculated MAVA states depend on the number of the 2^+ and 4^+ QRPA phonons included into the ansatz wave function (27) and the subsequent diagonalization of the eigenvalue problem. It is enough, according to our calculations, to take five lowest QRPA phonons of both of these multipoles to achieve stable energies and wave functions for the calculated MAVA states. This number of the QRPA phonons has been used for all the results presented here. These results concern the energies and $E2$ decay properties of the 2_1^+, 2_2^+, 0_1^+ and 4_1^+ excited states in the Mo, Ru and Cd chains of isotopes. The experimental data are taken from Refs. [51, 52, 53, 54, 55, 56, 57, 58, 59, 60, 61, 62, 63].

The two-phonon state energies are represented in Fig. 1. In the case of molybdenum isotopes the two-phonon states were hard to recognize from the experimental spectrum and thus they are not shown here. Figures showing possible candidates for two-phonon states can be found in the included paper **PIII**. The general trend in the case of ruthenium isotopes (left panel) is that the theoretical two-phonon states are too high in energy as compared to the experimental ones. Still the agreement is reasonable and the isotope ^{106}Ru is quite well reproduced even though the ordering of the states has changed. In the case of cadmium isotopes (right panel) all the theoretical two-phonon states are in good agreement with their experimental counterparts, excluding the $0^+_{2-\mathrm{ph}}$ states in the heaviest isotopes ^{118,120}Cd.

As already mentioned in the previous chapter, the metric matrix plays an important role also in the theoretical expressions for the electric decay amplitudes [50]. These amplitudes can be used to produce the reduced electric quadrupole decay probabilities, $B(E2)$, which can be compared with experimental data. To do this comparison we adopt proton and neutron effective charges, $e_{\mathrm{p}} = (1+\chi)e$ and

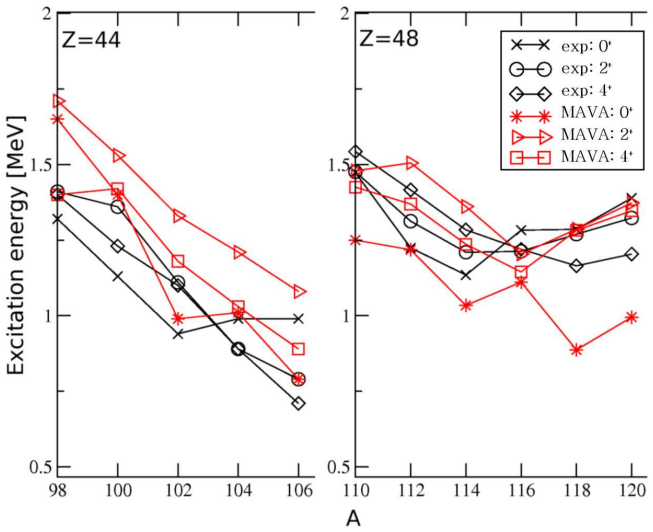

FIGURE 1: Experimental and theoretical two-phonon energies in $^{98-106}$Ru (left panel) and $^{110-120}$Cd isotopes (right panel).

$e_{\rm n} = \chi e$, which reproduce the measured $B(E2; 2_1^+ \to 0_{g.s.}^+)$ value. The electric polarization factor, χ, as well as the experimental $B(E2; 2_1^+ \to 0_{g.s.}^+)$ value are plotted in Fig. 2. General trend is that higher χ values are needed when $B(E2; 2_1^+ \to 0_{g.s.}^+)$ increases.

The electric quadrupole transition strengths are represented in Fig. 3 as ratios

$$R(J_i^+ \to J_f^+) = \frac{B(E2; J_i^+ \to J_f^+)}{B(E2; 2_1^+ \to 0_{g.s.}^+)}. \tag{65}$$

One should notice that the inaccuracy limits of experimental results are not shown here. However, they can be found in papers **PI**, **PII** and **PIII**. The very weak transition from 2^+ two-phonon state to 0^+ ground state is reproduced extremely well in all cases. In general, the theoretical transition $2_{2-\rm ph}^+ \to 2_1^+$ is found to be stronger than the experimental one except for the molybdenum isotopes where the correspondence is very good. On the other hand theoretical transition $4_{2-\rm ph}^+ \to 2_1^+$ is found to be weaker than the experimental one. Deeper analysis of level energies and $B(E2)$ values, carried out in the included papers, reveals that according to our calculations $^{94-100}$Mo are closer to anharmonic vibrators than deformed rotors. Furthermore, ^{100}Ru can be interpreted as being a transitional nucleus between the

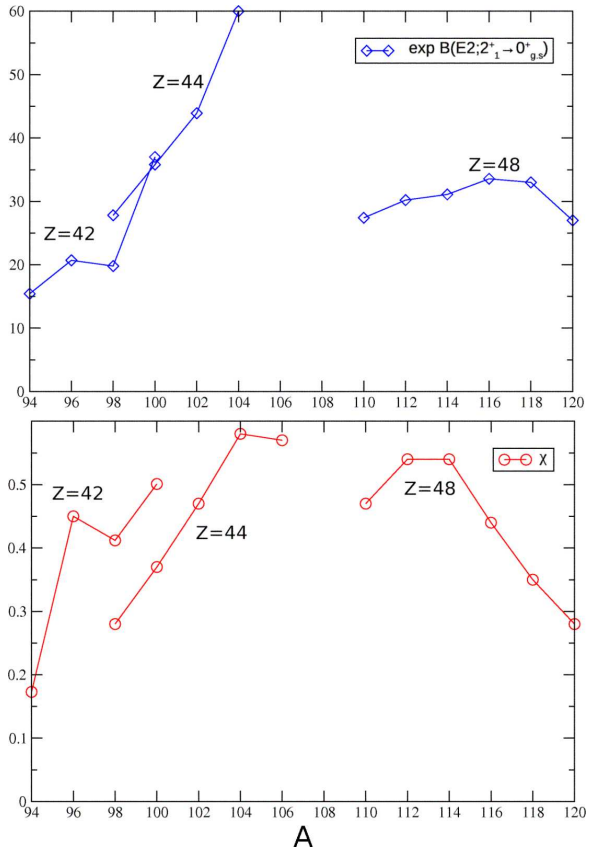

FIGURE 2: Experimental $B(E2; 2_1^+ \rightarrow 0_{g.s.}^+)$ values in Weisskopf units (upper panel) and the corresponding electric polarization factor, χ (lower panel) for $^{94-100}$Mo, $^{98-106}$Ru and $^{110-120}$Cd.

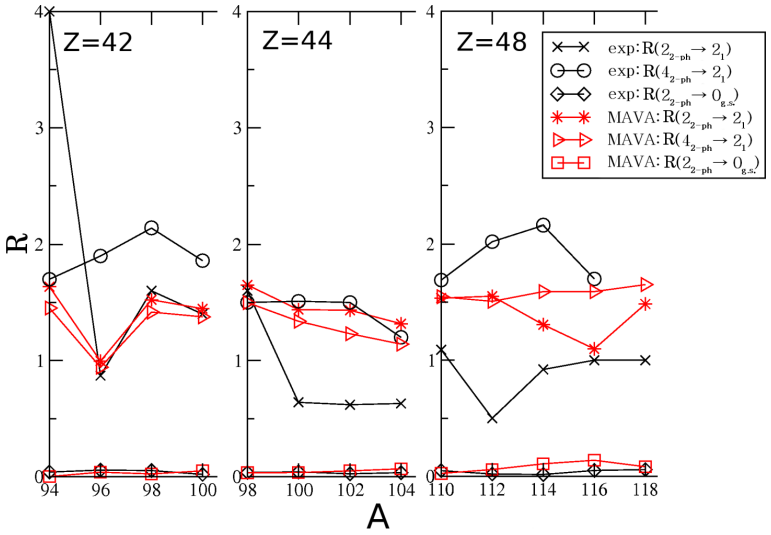

FIGURE 3: Experimental and theoretical ratios (65) values for some transitions for $^{94-100}$Mo (left panel), $^{98-106}$Ru (middle panel) and $^{110-120}$Cd (right panel).

spherical anharmonic vibrator ^{98}Ru and the quasi-rotational heavier $^{102-106}$Ru isotopes. In the case of $^{116-120}$Cd the analysis points to mixing between anharmonic vibrations and deformed intruder degrees of freedom.

5 LARGE SCALE CALCULATIONS

In the following sections large scale (global) calculations with MAVA are described. This study is very recent and has not been published yet. The goal of the calculations is to fix free parameters by experimental data so that a large region of nuclei could be studied with the same parameters. This is a very demanding task since the key issue here, and in general in nuclear-structure theory, is that no parameter-free, practically applicable many-body theory exists. The minimization method chosen is the NAG fortran E04FCF routine which is used together with the experimental data provided by the ensdf database in the simulations in order to fix the free parameters in an optimal, automatic way. For such calculations the MAVA has been modified to allow user friendly calculations globally by choosing the reasonable candidates from the entire chart of nuclei. Energies of the first excited 2^+ states of vibrational like doubly even nuclei are used as the first experimental data set to be studied. Preliminary results using a G-matrix as a two-body interaction are promising.

5.1 Minimization method

The NAG fortran E04FCF routine is used to minimize the difference between experimental and theoretical 2_1^+ energies. E04FCF is a comprehensive algorithm for finding an unconstrained minimum of a sum of squares of m nonlinear functions in n variables ($m \geq n$) using both Gauss–Newton and modified Newton algorithms. The routine is intended for functions which have continuous first and second derivatives, although it will usually work even if the derivatives have occasional discontinuities.

E04FCF is applicable to problems of the form

$$\text{Minimize } F(x) = \sum_{i=1}^{m} [f_i(x)]^2, \tag{66}$$

where $x = (x_1, x_2, ..., x_n)^T$ and $m \geq n$. Essentially E04FCF is identical to the subprogram LSQNDN in the National Physical Laboratory Algorithms Library. First the user supplies a starting point $x^{(1)}$ from where the routine generates a sequence of points $x^{(2)}, x^{(3)}, ...$ which is intended to converge to a local minimum of $F(x)$. The sequence of points is given by

$$x^{(k+1)} = x^{(k)} + \alpha^{(k)} p^{(k)} k, \tag{67}$$

where the vector $p^{(k)}$ is a direction of search, and $\alpha^{(k)}$ is chosen such that $F\ (x^{(k)} + \alpha^{(k)} p^{(k)})$ is approximately a minimum with respect to $\alpha^{(k)}$. The vector $p^{(k)}$ used depends on the reduction in the value of the sum of squares obtained during the last iteration. If the sum of squares was sufficiently reduced, then $p^{(k)}$ is an approximation to the Gauss-Newton direction. Otherwise additional function evaluations are made so as to enable $p^{(k)}$ to be a more accurate approximation to the Newton direction. The method is designed to ensure that steady progress is made whatever the starting point may be, and to have the rapid ultimate convergence of the Newton's method. More detailed description of the algorithm can be found in Ref. [64].

5.2 Calculations

First the choice of valence space has to be made. This also defines the region of nuclei to be calculated. In these calculations we have chosen the valence space $1p0f - 2s1d0g - 0h1f_{7/2}$ confining the proton numbers between $22 \leq Z \leq 64$ and neutron numbers between $22 \leq N \leq 74$. The nuclei that are taken under discussion are chosen by evaluating the $4_1^+/2_1^+$ ratio of experimental energies. In the present calculations the suitable experimental candidates are taken to be those with $1.5 \leq E(4_1^+)/E(2_1^+) \leq 2.5$.

Next the parameters to be fitted are chosen. In the present version the parameters that are fitted are the QRPA particle-hole parameter g_{ph}, the QRPA particle-particle parameter g_{pp} and the Woods-Saxon parameters: the strength of the central potential V_0, the range R and the surface thickness a. In the following the Woods-Saxon parameters are denoted by the symbols WS_i for the i:th parameter. The

strength of the central potential includes two parameters and is calculated as

$$V_0 = -(WS_4 \pm WS_5(N-Z)/A), \tag{68}$$

the $+$ sign being for protons and the $-$ sign for neutrons. The range can be obtained from

$$R = WS_2 A^{1/3} \tag{69}$$

and the surface thickness is simply $a = WS_3$. For the spin-orbit part one more parameter is needed for scaling its central strength

$$v_{ls} = WS_1 V_0. \tag{70}$$

The starting values for the parameters are $WS_1 = 0.44$, $WS_2 = 1.27$, $WS_3 = 0.67$, $WS_4 = -51.00$, $WS_5 = 33.00$, $g_{ph} = 0.60$ and $g_{pp} = 1.00$ and the final fitted parameters in each case are shown in Table 1. The first row indicates the parameter label and the following four rows show the fitted parameters in four different cases; MAVA calculations with five Woods-Saxon parameters, MAVA calculations with three Woods-Saxon parameters and the particle-hole parameter, MAVA calculations with three Woods-Saxon parameters, the particle-hole parameter and the particle-particle parameter, and for comparison a QRPA calculation with three Woods-Saxon parameters, the particle-hole parameter and the particle-particle parameter. The last line of the table shows the residues of the calculations, i.e., the minimized sum of squares of differences between the experimental and theoretical energy divided by the number of calculated nuclei.

From the calculation where only the Woods-Saxon parameters are fitted one can see that the most sensitive parameters are WS_1, WS_4 and WS_5. Thus these parameters are taken to be fitted with particle-hole and particle-particle parameters. Judging by the residue $\min F(x)/m$ the $WS + g_{ph} + g_{pp}$ calculation gives the best result. One also sees that taking into account the g_{ph} and g_{pp} parameters, the change in the Woods-Saxon parameters is decreased. In the case of the QRPA fit, the Woods-Saxon parameters remain almost untouched leading to the biggest residue.

The fitted energies are shown in Figures 4, 5 and 6. The experimental values are extracted from the ensdf database and are represented in the figures only if any of the theoretical counterparts could be calculated. At this point a general remark concerning these figures is in order. The QRPA energies of the 2_1^+ state are mainly determined by the g_{ph} parameter and no breakdown of the theory is expected for reasonable values of g_{ph}. Hence, for almost all nuclei included in our

TABLE 1: Fitted parameters of the global MAVA calculations. The asterisk marks values of parameters that are fixed in the calculations. The last line gives the residue of the calculations in units of keV.

		MAVA		QRPA
	WS	$WS + g_{ph}$	$WS + g_{ph} + g_{pp}$	$WS + g_{ph} + g_{pp}$
WS_1	0.4480	0.4400	0.44021	0.43999
WS_2	1.2697	1.27*	1.27*	1.27*
WS_3	0.66513	0.67*	0.67*	0.67*
WS_4	-51.7997	-51.0001	-51.0101	-51.0001
WS_5	28.5792	33.4911	32.9357	32.9880
g_{ph}	0.60*	0.5895	0.5719	0.5852
g_{pp}	1.00*	1.00*	1.0723	0.9378
$\frac{\min F(x)}{m}$	519.18	449.41	425.24	531.26

compilation the QRPA energy is found. On the other hand, the 2_1^+ energy of the MAVA not only depends on g_{ph} but also on the interaction between the 2_1^+ state and the two-phonon triplet. On many occasions this interaction pushes the 2_1^+ energy imaginary (breakdown of the MAVA formalism) even if the QRPA energy of the 2_1^+ phonon, the main component of the MAVA 2_1^+ state and the building block of the MAVA two-phonon triplet, is positive. Hence the MAVA breaks down in our global calculations more often than the QRPA does. Most pronounced this effect seems to be for the MAVA calculations with optimized WS, g_{ph} and g_{pp} parameters. In figures a missing theory point implies a breakdown of calculation.

It is interesting to see how the previously independently calculated molybdenum, ruthenium and cadmium isotopes are reproduced with fitted parameters. Before making any conclusions one should notice that the fitted g_{ph} parameters differ quite radically from the ones represented in the included papers. Fig. 5 shows the results for the $Z = 42 - 48$ nuclei. First look at the molybdenum isotopes, $Z = 42$ and $N = 52 - 58$, reveals that from the previously independently calculated isotopes only ^{100}Mo, $N = 58$, can be calculated with three fitted Woods-Saxon parameters and fitted g_{ph} and g_{ph} in the MAVA. For the $N = 52 - 56$ isotopes the calculation breaks down. However, the QRPA seems to give quite nice results for those isotopes.

In the case of the ruthenium isotopes, $Z = 44$ and $N = 54 - 62$, the calculation

with three fitted Woods-Saxon parameters and fitted g_{ph} is giving the best results for MAVA. The trend in all the calculations seems to be somewhat in the wrong direction, i.e., on the experimental side the energy of the first 2^+ state decreases as more neutrons are added but on the theoretical side the reverse happens.

Unfortunately only quite few of the previously independently calculated cadmium isotopes, $Z = 48$ and $N = 62 - 72$, can be calculated with the fitted parameters. The most neutron rich isotopes are, surprisingly enough, best reproduced by the five fitted Woods-Saxon parameters.

Another interesting feature in such large scale calculations is the reproduction of shell closures. Between the magic shell closures collective excitations of nucleons become evident in the form of vibrational and rotational states in their low-energy spectrum. These collective effects are expected to be strongest at midshell. However, the development of collectivity away from major shell closures may be disturbed by the presence of subshell closures, or minor shell gaps. In order to study such phenomena, indicators of quadrupole collectivity may be made use of. One measure of the amount of quadrupole collectivity in even-even nuclear systems is the energy of the first excited 2^+ state. According to [65, 66], the energy of the first 2^+ state, $E(2_1^+)$, is inversely proportional to the quadrupole deformation parameter. Thus, nearly spherical nuclei exhibit high $E(2_1^+)$ values relative to more deformed neighboring even-even isotopes. As nucleons are added to the system beyond closed major shells, $E(2_1^+)$ will decrease, a result of the dominance of collective motion among nucleons. The existence of subshells between major shell closures should result in similar $E(2_1^+)$ trends.

Fig. 4 shows the crossing of the $N = 28$ neutron shell. This shell closure is quite nicely reproduced by all the fits even though in general the theoretical energies are slightly too low. The calculations of Caurier *et al.* [67] suggest that there are possible intruder states around 500 keV in $N = 28$ isotones ^{50}Ti, ^{52}Cr and ^{54}Fe belonging to an yrare band. However, they do not seem to show up experimentally. On the other hand in the shell-model diagonalization calculation of [68] the theoretical 2_1^+ state is found to be higher in energy than the experimental one in the nuclei ^{50}Ti, ^{52}Cr and ^{54}Fe.

In their paper Prisciandaro et al. [69] discuss a possible subshell closure at $N = 32$ seen in Cr isotopes. These heavier Cr isotopes are not included in our calculations since they do not have vibrational features judging by the $4_1^+/2_1^+$ energy ratio.

As shown by the last panel of the first row of panels in Fig. 4 a subshell

closure at $N = 40$ is seen experimentally for ^{68}Ni but it is not reproduced by our calculation. However, the $WS + g_{ph} + g_{pp}$ calculation seems to have the right trend in the energies. This seems to be a hard subshell closure to reproduce since the shell-model calculation of Ref. [70] is also not able to reproduce it.

Fig. 6 shows that the theoretical energies of a chain of isotopes vary quite radically when adding more neutrons. This effect could possibly be diminished by taking the g_{ph} and g_{pp} parameters to be functions of A and Z. Thus more calculations should be done to find the most suitable form for the functions $g_{ph}(A, Z)$ and $g_{pp}(A, Z)$.

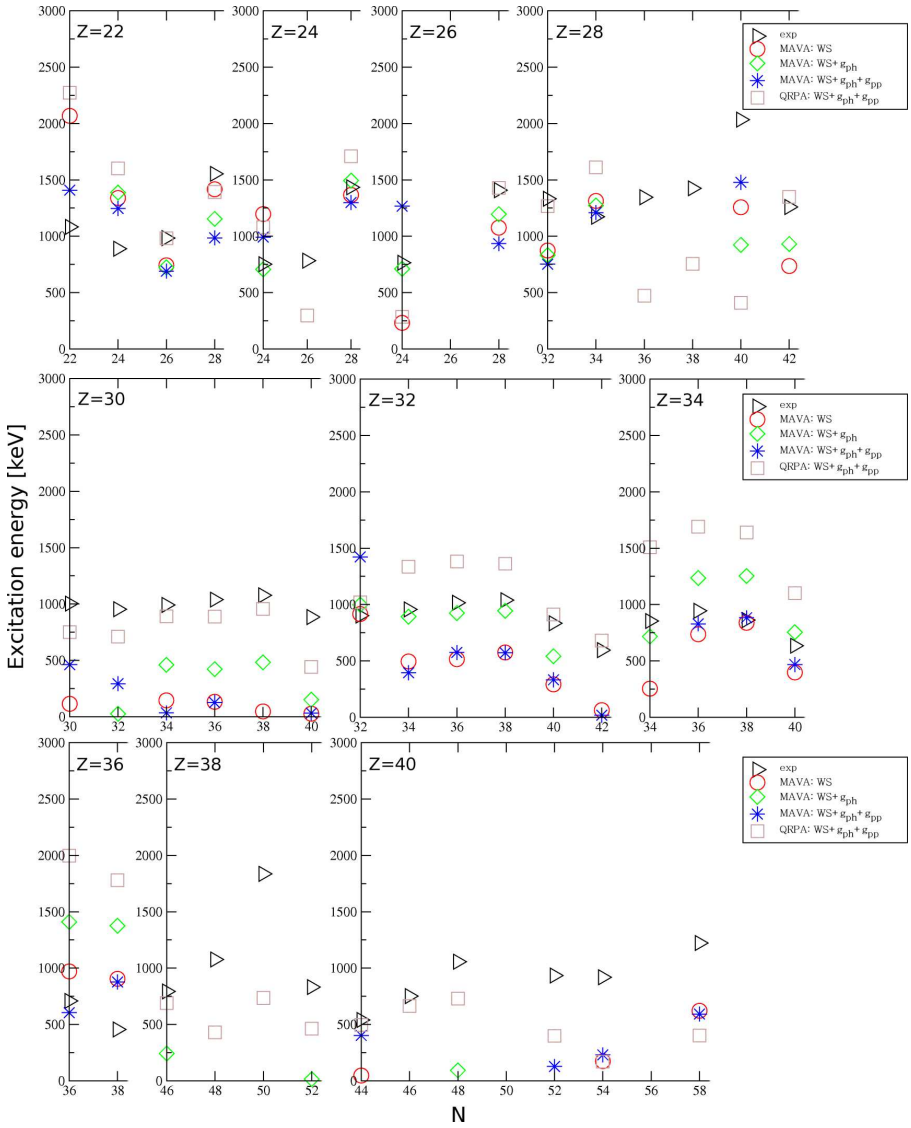

FIGURE 4: Energies of the first 2^+ states calculated with the fitted parameters for $Z = 22 - 40$ nuclei as functions of the neutron number. Z increases from left to right and the first row of panels corresponds to $Z = 22 - 28$, the second row to $Z = 30 - 34$ and the third row to $Z = 36 - 40$.

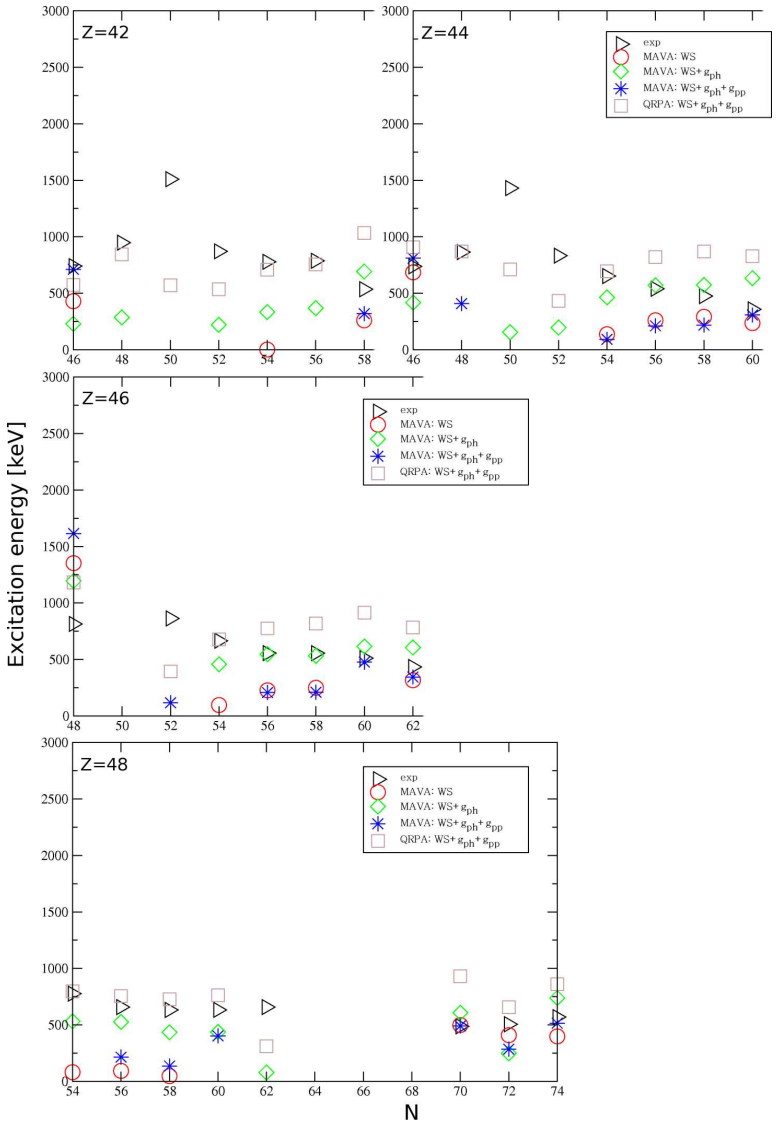

FIGURE 5: Energies of the first 2^+ states calculated with the fitted parameters for $Z = 42 - 48$ nuclei as functions of the neutron number. Z increases from left to right and the first row of panels corresponds to $Z = 42, 44$, the second row to $Z = 46$ and the third row to $Z = 48$.

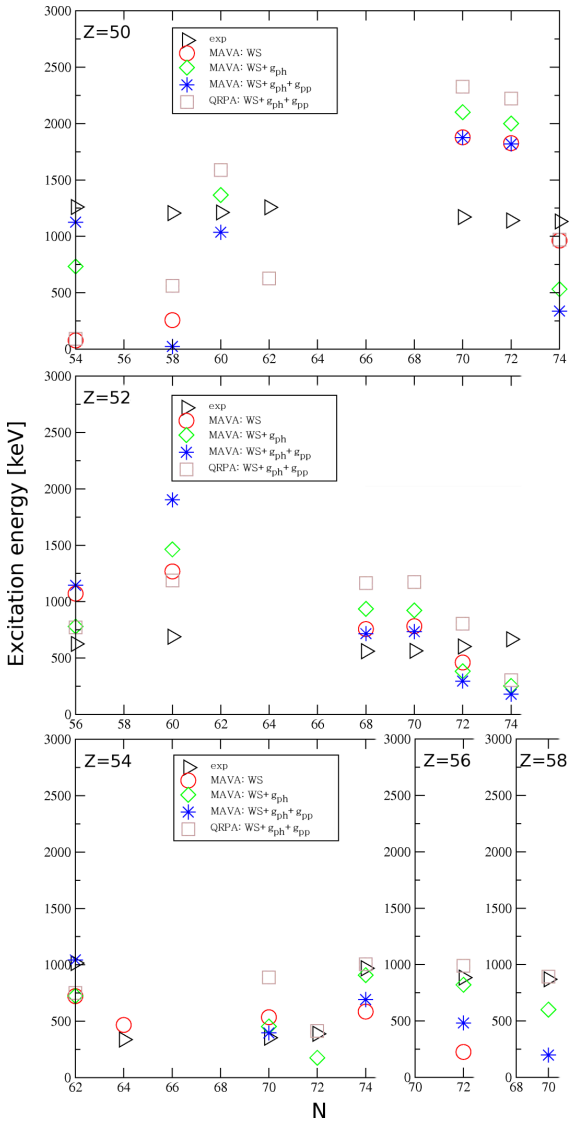

FIGURE 6: Energies of the first 2^+ states calculated with the fitted parameters for $Z = 50 - 58$ nuclei as functions of the neutron number. Upper panel corresponds to $Z = 50$, the middle panel to $Z = 52$ and the lowest row of panels to $Z = 54 - 58$.

6 CONCLUSIONS

The adopted theory of this work, MAVA, is based on a large single-particle valence space and a realistic microscopic Hamiltonian, using phenomenologically renormalized two-body interaction based on the Bonn one-boson-exchange potential. The nuclear Hamiltonian is diagonalized in a basis containing one-phonon and two-phonon components, coupled to a given angular momentum and parity. By its two-step procedure MAVA is a simple representative of the multistep shell model. The improved version, MAVA2, also considers properly the fermionic structure of the QRPA phonons and goes beyond the quasiboson approximation in the commutators.

In our present calculations the two-phonon basis is built using 2^+ and 4^+ QRPA eigenstates. In spite of its simplicity, the model predicts energies and ratios of $B(E2)$ values in reasonable agreement with data. Furthermore, based on the obtained results identification of three-phonon states and intruder states can be made. Also evidence of shape transitions and shape coexistence can be seen. Thus MAVA is a versatile tool in studying spherical and nearly spherical nuclei with low-lying collective vibrational like states. In addition to the description of electric quadrupole decays further applications are the descriptions of beta decay and double-beta decay transitions within the proton-neutron version of MAVA [71].

The large scale (global) calculations with MAVA are done in the aim to fix the free parameters by experimental data so that a large region of nuclei could be studied with the same parameters. The first experimental data set studied are the energies of the first excited 2^+ states of vibrational like doubly even nuclei. Preliminary results of these calculations using a G-matrix as a two-body interaction are promising and could already be used to calculate various properties of two-phonon states. Improvement of the results could be accomplished by taking the g_{ph}

and g_{pp} parameters to be functions of A and Z and finding the most suitable form for the functions $g_{ph}(A, Z)$ and $g_{pp}(A, Z)$, thus requiring more calculations.

REFERENCES

[1] A. Arima and F. Iachello, Adv. Nucl. Phys. **13** (1984) 139.

[2] D.J. Rowe, *Nuclear Collective Motion* (Methuen, London, 1970).

[3] P. Ring and P. Schuck, *The Nuclear Many-Body Problem* (Springer-Verlag, Berlin, 1980).

[4] P. Ring and P.Schuck, Phys. Rev. C **16** (1977) 801, and references therein.

[5] R.J. Liotta and C. Pomar, Nucl. Phys. A **382** (1982) 1.

[6] C. Pomar, J. Blomqvist, R.J. Liotta and A. Insolia, Nucl. Phys. A **515** (1990) 381.

[7] A. Insolia, N. Sandulescu, J. Blomqvist and R.J. Liotta, Nucl. Phys. A **550** (1992) 34.

[8] B. Silvestre-Brac and R. Piepenbring, Phys. Rev. C **26** (1982) 2640.

[9] M. Grinberg, P. Piepenbring, K.V. Protasov and B. Silvestre-Brac, Nucl. Phys. A **597** (1996) 355.

[10] K.V. Protasov, B. Silvestre-Brac, R. Piepenbring and M. Grinberg, Phys. Rev. C **53** (1996) 1646.

[11] K.V. Protasov and R. Piepenbring, Nucl. Phys. A **632** (1998) 39.

[12] F. Andreozzi *et al.*, Phys. Rev. C **75** (2007) 044312.

[13] V.G. Soloviev, *Theory of Atomic Nuclei: Quasiparticles and Phonons* (IOP publishing, Bristol, 1992).

[14] U. Kneissl, H.H. Pitz and A. Zilges, Prog. Part. Nucl. Phys. **37** (1996) 439.

[15] N. Lo ludice and Ch. Stoyanov, Phys. Rev. C **62** (2000) 047302.

[16] N. Lo ludice and Ch. Stoyanov, Phys. Rev. C **65** (2002) 064304.

[17] V.G. Soloviev, A.V. Sushkov, N.Yu. Shirikova and N. Lo ludice, Nucl. Phys. A **600** (1996) 155.

[18] T. Auman, P.F. Bortignon and H. Hemling, Annu. Rev. Nucl. Part. Sci. **48** (1998) 351.

[19] C.A. Bertulani and V.Yu. Ponomarev, Phys. Rep **321** (1999) 139.

[20] V.Yu Ponomarev P.F. Bortignon, R.A Broglia and V.V. Voronov, Phys. Rev. Lett. **85** (2000) 1400.

[21] S. Drozdz, S. Nishizaki, J. Speth and J. Wambach, Phys. Rep. **197** (1990) 1.

[22] M. Tohyama and P. Schuck, Eur. Phys. J. A **19** (2004) 203.

[23] K.L.G. Heyde, *The Nuclear Shell Model, second edition* (Springer-Verlag, 1994).

[24] A. Bohr and B.R. Mottelson, *Nuclear Structure, Vol I: Single-particle Motion* (Benjamin, New York, 1969).

[25] M.G. Mayer, Phys. Rev. **78** (1950) 16.

[26] M.G. Mayer, Phys. Rev. **78** (1950) 22.

[27] I. Talmi, Nucl. Phys. A **172** (1971) 2.

[28] K. Allaart, E. Boeker, G. Bonsignori, M. Savoia and Y. K. Gambhir, Phys. Rep. **169** (1988) 209.

[29] J. Bardeen, L.N. Cooper and J.R. Schrieffer, Phys. Rev. **108** (1957) 1175.

[30] A. Bohr, B.R. Mottelson and D. Pines, Phys. Rev. **110** (1958) 936.

[31] N.N. Bogoliubov, J. Exptl. Theoret. Phys. **34** (1958) 58.

[32] N.N. Bogoliubov, Nuovo Cimento **7** (1958) 794.

[33] J.G. Valatin, Nuovo Cimento **7** (1958) 843.

[34] M. Baranger, Phys. Rev. **120** (1960) 957.

[35] D.J. Rowe, Rev. Mod. Phys. **40** (1968) 153.

[36] A.M. Lane, Nuclear Theory (Benjamin, New York, 1964).

[37] S. Kislinger and R.A. Sorensen, Mat. Fys. Medd. **32** (1960) No.9.

[38] S. Yoshida, Phys. Rev. **123** (1961) 2122.

[39] D.S. Delion and J. Suhonen, Phys. Rev. C **64** (2001) 064302.

[40] A. Klein and E.R. Marshalek, Rev. Mod. Phys. **63** (1991) 375.

[41] D.S. Delion and J. Suhonen, Phys. Rev. C **61** (2000) 024304.

[42] G. Racah, Phys. Rev. **62** (1942) 483.

[43] J. Suhonen, From Nucleons to Nucleus; Concepts of Microscopic Nuclear Theory, (Springer, Berlin, 2007).

[44] F. Catara, Ph. Chomaz and N. Van Giai, Phys. Lett. B **277** (1992) 1.

[45] K. Holinde, Phys. Rep. **68** (1981) 121 .

[46] J. Suhonen and O. Civitarese, Phys. Lett. B **497** (2001) 221.

[47] J. Suhonen, T. Taigel and A. Faessler, Nucl. Phys. A **486** (1988) 91.

[48] J. Suhonen, Nucl. Phys. A **563** (1993) 205.

[49] G. Audi and A.H. Wapstra, Nucl. Phys. A **565** (1993) 1.

[50] D.S. Delion and J. Suhonen, Phys. Rev. C **67** (2003) 034301.

[51] J.K. Tuli, Nucl. Data Sheets **66** (1992) 1.

[52] L.K. Peker, Nucl. Data Sheets **68** (1993) 165.

[53] B. Singh, Nucl. Data Sheets **81** (1997) 1.

[54] B. Singh, Nucl. Data Sheets **84** (1998) 565.

[55] J. Blachot, Nucl. Data Sheets **64** (1991) 1.

[56] D. De Frenne and E. Jacobs, Nucl. Data Sheets **72** (1994) 1.

[57] D. De Frenne and E. Jacobs, Nucl. Data Sheets **83** (1998) 535.

[58] N. Sandulescu, A. Insolia, B. Fant, J. Blomqvist and R.J. Liotta, Phys. Lett. B **288** (1992) 554.

[59] D. De Frenne and E. Jacobs, Nucl. Data Sheets **89** (2000) 534.

[60] D. De Frenne and E. Jacobs, Nucl. Data Sheets **79** (1996) 668.

[61] J. Blachot and G. Margueir, Nucl. Data Sheets **75** (1995) 99.

[62] K. Kitao, Nucl. Data Sheets **75** (1995) 99.

[63] J. Blachot, Nucl. Data Sheets **92** (2001) 473.

[64] P. E. Gill and W. Murray, SIAM J. Numer. Anal. **15** (1978) 977.

[65] L. Grodzins, Phys. Lett. **2** (1962) 88.

[66] F.S. Stephens *et al.*, Phys. Rev. Lett. **29** (1972) 438.

[67] E. Caurier *et al.*, Nucl. Phys. A **742** (2004) 14.

[68] T. Mizusaki *et al.*, Phys. Rev. C **63** (2001) 044306.

[69] J.I. Prisciandaro *et al.*, Phys. Lett. B **510** (2001) 1723.

[70] J. Van de Walle *et al.*, Phys. Rev. Lett. **99** (2007) 142501.

[71] D.S. Delion and J. Suhonen, Nucl. Phys. A **781** (2007) 88.